PNNL-11639
UC-2030

Pacific Northwest
National Laboratory

Operated by Battelle for the
U.S. Department of Energy

Initial Parametric Study of the Flammability of Plume Releases in Hanford Waste Tanks

Z. I. Antoniak
K. P. Recknagle

August 1997

Prepared for the U.S. Department of Energy
under Contract DE-AC06-76RLO 1830

PNNL-11639

DISCLAIMER

PACIFIC NORTHWEST NATIONAL LABORATORY
operated by
BATTELLE
for the
UNITED STATES DEPARTMENT OF ENERGY
under Contract DE-AC06-76RLO 1830

Printed in the United States of America

Available to DOE and DOE contractors from the Office of Scientific and Technical Information, P.O. Box 62, Oak Ridge, TN 37831; prices available from (615) 576-8401.

Available to the public from the National Technical Information Service, U.S. Department of Commerce, 5285 Port Royal Rd., Springfield, VA 22161


This document was printed on recycled paper.

PNNL-11639
UC-2030

Initial Parametric Study of the Flammability of Plume Releases in Hanford Waste Tanks

Z. I. Antoniak
K. P. Recknagle

August 1997

Prepared for
the U.S. Department of Energy
under Contract DE-AC06-76RLO 1830

Pacific Northwest National Laboratory
Richland, WA 99352

Summary

This study comprised systematic analyses of waste tank headspace flammability following a plume-type of gas release from the waste. First, critical parameters affecting plume flammability were selected, evaluated, and refined. As part of the evaluation the effect of ventilation (breathing) air inflow on the convective flow field inside the tank headspace was assessed, and the magnitude of the so-called "numerical diffusion" on numerical simulation accuracy was investigated. Both issues were concluded to be negligible influences on predicted flammable gas concentrations in the tank headspace. Previous validation of the TEMPEST code against experimental data is also discussed, with calculated results in good agreement with experimental data.

Twelve plume release simulations were then run, using release volumes and flow rates that were thought to cover the range of actual release volumes and rates. The results indicate that most plume-type releases remain flammable only during the actual release itself, and only a very small fraction of the total release volume is flammable at any instant. Mixing in the tank headspace is so rapid that the potential for a flammable concentration ceases as soon as the release ends. Only for very large releases representing a significant fraction of the volume necessary to make the entire mixed headspace flammable (many thousands of cubic feet) can flammable concentrations persist for several hours after the release ends. However, as in the smaller plumes, only a fraction of the total release volume is flammable at any one time. The transient evolution of several plume sizes is illustrated in a number of color contour plots that provide insight into plume mixing behavior.

Contents

Figures

Tables

1.0 Introduction

A gas release is termed a "plume release" for the purposes of this report if it represents a localized event whose volume does not exceed the lower flammability limit (LFL) when fully mixed with the ambient headspace atmosphere, although the gas is flammable as it exits the waste. Only a few of the large gas releases in Tank 241-SY-101 prior to mixing were known to be of sufficient volume to make the entire tank headspace flammable. The smaller volumes released from the five double-shell tanks (DSTs) currently exhibiting episodic gas release events (GREs) all classify as plume releases, as do the much smaller local releases observed in some of the single-shell tanks (SSTs) with gas monitors installed.

The main issues concerning plume releases are how long a plume remains flammable and what gas volume is flammable at any given time. The plume begins being diluted with the surrounding air by molecular diffusion and turbulent mixing as soon as it leaves the waste surface. We expect that only a small fraction of the total release volume is ever flammable and that flammable conditions exist for a relatively short period of time. This report presents the results of a series of detailed, three-dimensional computational simulations that follow the evolution of the plume to track the flammable volume as a function of time.

Various plume-type gas releases in both DSTs and SSTs have been modeled in the past. However, this modeling had a specific purpose: to match measured concentrations of hydrogen observed during a GRE. The present study of plume-type GREs is non-specific but attempts to systematically probe the parameters of both measured and postulated releases. Because both the number of parameters and their range are large, we restricted simulation parameters to those most likely to affect plume dispersion within the headspace.

These simulations were performed with the TEMPEST hydrothermal computer code. TEMPEST is a semi-implicit, finite-difference model that solves the time-dependent, three-dimensional mass, momentum, and energy conservation equations for incompressible flows (Trent and Eyler 1991). Momentum equations include explicit advection and implicit shear stress; the continuity and pressure solutions are both implicit. The solutions to scalar equations (energy, turbulence, constituent, electromotive force) are also implicit; energy transport and electromotive force are solved for both fluid and solid regions.

Section 2 of this report describes the selection of the important parameters to be varied and an evaluation of the appropriate ranges of these parameters. Section 3 summarizes the parameters and ranges actually selected for the simulation matrix. The results of the study are given in Section 4, along with specific conclusions and recommendations. Cited references are provided in Section 5.

2.0 Parameter Selection and Range Evaluation

The most significant parameters affecting plume flammability were selected based on previous simulations, which are listed in Table 2.1; additional computer modeling of mechanisms affecting dispersion; hand calculations; and engineering judgment. Appropriate parameter ranges were similarly determined by examining prior simulations, tank monitoring data, and safety analyses. Three categories of parameters were identified:

- Plume characteristics such as release volume, hydrogen fraction, release duration, and the initial velocity of the plume as it exits the waste.
- Geometry such as release location, flow area, and tank headspace (dome) volume.
- Factors affecting the internal flow field such as in-tank and ambient thermal conditions, location and size of vents, and barometric pressure variations.

Each of these categories is discussed separately, evaluating the relevance and magnitude of the parameters contained therein.

Table 2.1. Summary of Relevant Past TEMPEST Simulations

Reference note #	Tank(s) simulated[a]	H_2 Release Volume m^3 (ft^3)	Release duration, min	Max. H_2 concentration, %	Parameters examined
(b)	S-108; SY-101	9.63 (340)[c]	2	<2.5[d]	Flow field; release location
(e)	S-108	9.63 (340)[c]	2	2.8[d]	H_2 fraction; plume velocity
(f)	AW-101	8.50 (300)	120	0.89[g]	H_2 concentration matching; location; ambient temperature
(h)	AN-105	14.2 (500)	10	1.66[g]	H_2 conc. matching

(a) Tanks are officially identified with the prefix 241-. In this report the 241- has been omitted, as it is in common usage.
(b) Antoniak ZI and KP Recknagle. 1996. *Modeling Hydrogen Plume Concentrations in Single- and Double-Shell Tank Domes.* TWSFG96.12, PNNL, Richland, Washington.
(c) Simulated plumes were mixtures with a fixed volume of H_2 (LANL 1995, *A Safety Assessment for Salt-Well Pumping Operations in Tank 241 A-101: Hanford Site, Richland, Washington* [draft]) and a varying volume of air, equaling from 0 to 900% of the volume of H_2 (additional).
(d) After release ended.
(e) Antoniak ZI and KP Recknagle. 1996. *Modeling Hydrogen Plume Concentrations in a Single-Shell Tank Dome.* TWSFG96.6, PNNL.
(f) Antoniak ZI and KP Recknagle. 1995. *Modeling Post-GRE Spatial and Temporal Hydrogen Concentrations in Tank 241-101-AW Dome.* PNLFG:080295, PNNL.
(g) Simulation matched measured maximum concentration during GRE (Wilkins 1996).
(h) Antoniak ZI and KP Recknagle. 1996. *Modeling Post-GRE Spatial and Temporal Hydrogen Concentrations in the Tank 241-AN-105 Dome.* WTSFG95.56, PNNL.

2.1 Plume Characteristics

The parameters associated with a particular plume have a direct influence on hydrogen concentrations during and after the release. Release volume, the hydrogen fraction of the gas released from the waste, the duration of the release, and velocity of the gas as it exits the waste are important. The release volume and hydrogen fraction define the total volume of hydrogen available to create a flammable condition. The release duration and gas velocity describe the intensity of the plume, which affects the fraction of the release that is flammable and how long flammability might persist after the release ends.

2.1.1 Plume Volume

The maximum hydrogen release volume in DSTs other than Tank SY-101 during historical GREs is about 14 m^3 (500 ft^3) (Stewart et al. 1996; Johnson et al. 1997, pp. 4–14). For example, the GRE of August 21, 1995, in Tank AN-105 that resulted in a measured 1.7% hydrogen concentration was calculated to be caused by a 14.2 m^3 (500 ft^3) hydrogen release that made up 43% of the total release volume (see Table 2.1). A recent GRE in Tank AW-101 released a somewhat smaller 9.6 m^3 (300 ft^3) of hydrogen (again, see Table 2.1). Before it was mitigated by mixing in late 1993, SY-101 had much larger releases. For example, during Event E in December 1991, 12,000 ft^3 of gas containing 4,000 ft^3 of hydrogen were estimated to have been released (Allemann et al. 1994, p. 1.7).

Continuous headspace hydrogen monitoring data have been available for SSTs only in the last few years. These data show that releases typically contain $\leq$1 m^3 (35 ft^3) of hydrogen (Wilkins et al. 1997, p. 15) and frequently occur during extreme barometric lows. The barometric low of December 12, 1995 (the barometer dropped ~1.7 kPa [0.25 psi]) resulted in a release in Tank U-103 of 0.5 m^3 (18 ft^3) of hydrogen. The maximum barometric change measured at Hanford is on the order of 6.90 kPa (1 psi) (see subsection 2.1.3.3); even if one were to linearly extrapolate the observed U-103 release to 6.90 kPa (1 psi), only ~2 m^3 (70 ft^3) of hydrogen would be involved. Others also have evaluated the GRE potential of SSTs and concluded that rates greater than 10 ft^3/min and volumes larger than 500 ft^3 are highly unlikely (LANL 1996).

A "steady-state," non-GRE type of release rate that approximately equals the hydrogen gas generation rate can be postulated for many tanks. For DST SY-101 it equals approximately 0.85 m^3 (30 ft^3) of hydrogen per day;[(a)] for most SSTs it is <0.1 m^3 (3 ft^3) of hydrogen per day (Wilkins et al. 1997, p. 37). Although these types of releases are hardly plumes in the usual sense of the term, they also will be simulated to determine the prevailing chronic condition in most SSTs.

2.1.2 Hydrogen Fraction

The hydrogen fraction of the gas released from the waste is variable but typically is over 30% hydrogen by volume. Recent measurements using the retained gas sampler (RGS) indicate the DST waste contains 32–62% hydrogen (Shekarriz et al. 1997). RGS tests in SSTs show a wider range of 14–75%.[(b)]

(a) Panisko FE, ZI Antoniak, WB Gregory, GM Koreski, JA Lechelt, CP Shaw, and NE Wilkins. October 31, 1996. *Quarterly Review of SY-101 Mixer Pump Data.* PNNL, Richland, Washington.

(b) RGS results for Tank A-101 are shown in Shekarriz et al. (1997). Preliminary RGS data for U-103, S-106, and SY-109 are given in PNNL letter reports TWSFG97.40, TWSFG97.47 and TWSFG97.62, respectively.

Previous simulations have investigated the effect of the hydrogen fraction by keeping the hydrogen volume constant and diluting it with varying volumes of air (see Table 2.1). These simulations showed that hydrogen fraction did not strongly influence plume behavior or flammability. Therefore, this parameter was not extensively modeled, and a fixed value of 40% hydrogen was chosen to represent typical conditions.

2.1.3 Plume Release Velocity

The influence of initial plume velocity to a maximum of about 8.23 m/s (27 ft/sec) has been studied in prior simulations.[a] The resultant hydrogen concentrations were found to be relatively unchanged by plume velocities. The reason for this is apparent from Figure 2.1, which shows rapid plumes decelerating by momentum exchange and slow plumes accelerating due to buoyancy, all trending to ~3.66 m/s (12 ft/sec). Unfortunately, the total buoyancy was not kept constant in these simulations, so some additional studies are necessary to fully elucidate plume velocity effects.

2.1.4 Plume Release Location

Actual GREs in tanks occur at random locations. The influence of initial release location has been investigated in earlier simulations,[b] and, except for early in the release, the resulting hydrogen concentrations were found to be relatively unaffected by the location of the plume release point. Therefore, all releases are conservatively assumed to occur near the tank wall.

2.1.5 Release Area

The area of the release, or plume base cross-sectional area, is an important parameter in plume dispersion. Based on video of the waste surface in DST SY-101, this area can range from a minimum of ~0.093 m^2 (1 ft^2) for a "fumarole" formation to a maximum of ~93 m^2 (1000 ft^2) in a large historical buoyant displacement GRE. An appropriate range for SSTs might be somewhat more restricted than that for SY-101 because of the smaller amount of hydrogen generated and released by SSTs.

2.1.6 Tank Headspace Volume

The free volume (also known as headspace, or dome volume) in Hanford waste tanks ranges between ~850 m^3 (30,000 ft^3) and >2266 m^3 (80,000 ft^3) (Hodgson at al. 1996). We have already developed and exercised a model of SST S-108, which has a headspace of ~2266 m^3 (80,000 ft^3), and this model was selected for use in all the plume release simulations that follow (see Section 4) as representative of SSTs. A finely detailed model of the SST S-102 headspace (see Section 2.2.3) was used specifically for examining headspace flow perturbations.

(a) Antoniak ZI and KP Recknagle. 1996. *Modeling Hydrogen Plume Concentrations in a Single-Shell Tank Dome*. TWSFG96.6, PNNL, Richland, Washington.

(b) Antoniak ZI and KP Recknagle. 1996. *Modeling Hydrogen Plume Concentrations in Single- and Double-Shell Tank Domes*. TWSFG96.12, PNNL, Richland, Washington.

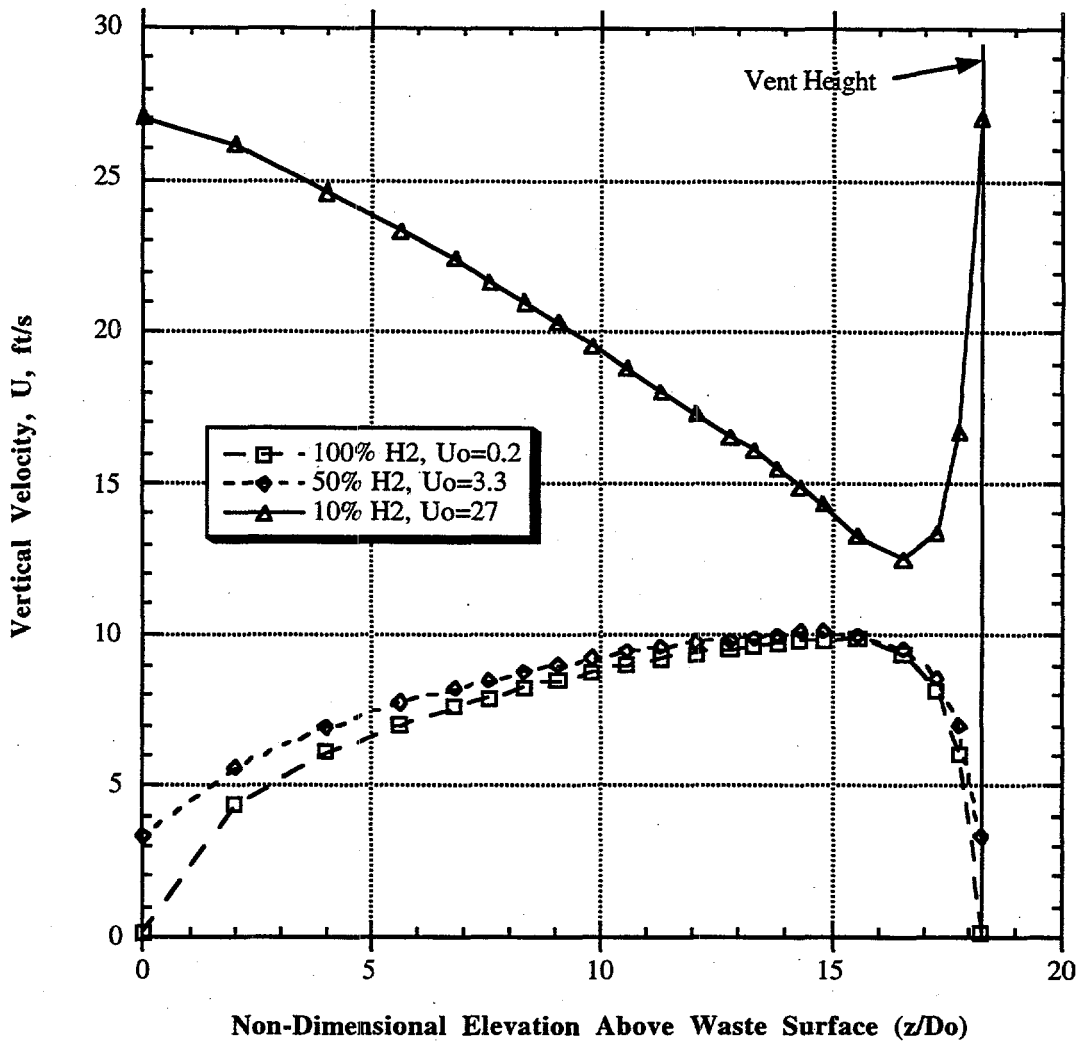

Figure 2.1. Effect of Initial Velocity on Plume Centerline Velocity

2.2 Plume Dispersion Mechanisms

Dispersion of a plume into its surroundings is a complex mixing process that occurs on several scales. On the microscale, mixing takes place by diffusion due to the random motion of both solute and solvent molecules. Much more rapid local mixing is a product of turbulence that may exist in the steady-state convective flow in the headspace or that may be generated by a buoyant plume as it rises. Finally, dispersion on the scale of the headspace dimensions occurs by thermal convection, which prevents formation and persistence of stratified layers that might remain flammable. The latter mechanism dominates the plume dispersion process.

Ventilation (and intertank flow through cascade lines) is a separate effect not directly related to plume dispersion inside the headspace. It can only add to dispersion to the extent that it influences the existing circulation within the headspace. Calculations are described below to show that it does not. The most important effect of ventilation is that it dilutes the hydrogen concentration in the headspace by removing it and replacing it with air at some rate. Typical passive ventilation rates are less than ~20 cfm (Wilkins et al. 1997); thus it would require more than three days to replace a headspace volume of 80,000 ft^3. A typical active ventilation system running at 200 cfm replaces the headspace volume in about seven hours. The time scales used in this study (10 minutes to two hours) make the effect of ambient air dilution negligible in passively ventilated tanks but might have a minor influence in actively ventilated tanks for the larger releases studied. We chose to conservatively ignore ventilation and cross flow except to show that it does not perturb the dominant natural convection flow field.

2.2.1 Diffusion

Even in gases, molecular diffusion is a relatively slow process. The diffusion coefficient for hydrogen in air is 0.611 cm^2/s (6.58E-4 ft^2/sec) at 273K (Cussler 1984, p. 106). Assuming diffusion is the only mechanism for dispersion, a stratified layer with a thickness of half the typical headspace height of 5 m and a hydrogen concentration of 8% would be reduced below 4%, the LFL for upward flame propagation, in about 15 hours. Most other mechanisms provide much faster mixing than this, as is shown in the following sections. Nevertheless, diffusion is included in the simulations because it is a physical mechanism that is easily modeled.

2.2.2 Turbulent Mixing

Turbulent flow is chaotic, with a secondary fluctuating flow comprising eddies at right angles to, and superimposed on, the main flow. This results in a continuous transport of energy, mass, and momentum from the main flow that greatly increases the mixing rate. Turbulence can therefore also be viewed as a large apparent increase in the viscosity and diffusivity of the main flow; this concept is frequently used in developing turbulence models and correlations.

The Reynolds numbers associated with large plume releases in DSTs are generally around 1,000, based on an assumed initial plume diameter. Such a plume would probably not be turbulent as it exits the waste, but buoyancy would probably induce turbulence at some distance above the waste surface. Very large, fast releases through small-diameter openings might approach a Reynolds number of 10,000, indicating that the plume is turbulent as it exits the waste surface, independent of buoyancy. The Reynolds number of the background thermal convection flow (discussed below) is on the order of ~20,000. Thus the pre-existing headspace atmosphere is likely to be turbulent without any help from the plume.

The enhanced mixing associated with this turbulence will begin to disperse the hydrogen release as soon as it exits the waste. However, the dominant length scale of the headspace convective turbulence is much larger than a computational cell, and most of the important effects are expected to be captured by mean flow-field simulation. Also, turbulent eddies created in a buoyant plume transfer very little momentum (Tenekes and Lumley 1972) and should not have an important effect on the pre-existing flow field. Based on these analyses, and for conservatism, we have elected to not use the turbulent mixing model in TEMPEST for the plume analyses that follow. It should be noted that turbulence was successfully included in the validation studies of a smaller-scale buoyant jet, as discussed in Section 4.

2.2.3 Thermal Convection in the Headspace

Thermal convection is the dominant mechanism by which SSTs and most DSTs transfer heat from the waste to the tank walls and thence to the atmosphere through the soil over the tank. In DSTs, cooling of the tank bottom by annulus ventilation flow may also be a significant heat sink, although less so than headspace convection.

Thermal convection is driven by the heat generated in the waste. The waste temperature is higher than that of the headspace, which is in turn higher than that of the tank walls. The air next to the waste is heated and rises to the tank dome, where it cools and sinks. This establishes large-scale convective cells that keep the headspace atmosphere nearly isothermal.

Earlier modeling and flow visualization studies investigated the effect of temperature difference between the waste surface and the dome atmosphere on the flow field. These studies showed that, even for the smallest difference examined (0.9°C [2°F]), convective velocities were on the order of tenths of a foot per second. Such velocities are enough to rapidly disperse any stratified layer of hydrogen that might form during the release; i.e., a tank headspace becomes fully mixed within about an hour after the cessation of a hydrogen plume release.[(a)]

2.2.3.1 Seasonal Variations

The seasonal variations in ambient outside air temperature can affect thermal convection in the headspace. As the tank "breathes," it ingests air at the current outside temperature. Also, the temperature of the soil that surrounds the buried tank and therefore exchanges heat with the headspace air varies seasonally. The first effect is small for SSTs, because they breathe only on the order of several cubic feet per minute. Even in the DSTs, for which we have studied high ventilation flow rates and temperature extremes of 20 and 120°F, ventilation has been found to exert only a minimal influence on internal convection patterns responsible for hydrogen dispersion in the headspace (see Table 2.1). Therefore, only the second issue is addressed, briefly, below.

Most SSTs have relatively cool waste, so the temperature of the dome atmosphere is only slightly above average ambient temperature.[(b)] During an extended hot weather period in late summer, it is postulated that hot air could collect in the upper portion of the dome, suppressing global convection in the headspace. The dispersion of any plume that entered such a layer would be limited to molecular diffusion, which would maintain high hydrogen concentrations for a much longer time than if convection were active.

The formation of a thermally stratified layer requires the inside surface temperature of the tank dome to be at or above the temperature of the air. If the surface is cooler, a downward convective flow will establish itself and disperse any stratification that might have developed.

Figure 2.2 shows the results of a hand calculation that was performed to evaluate the transient subsoil temperature profile that might exist above an SST. As expected, the soil at tank dome depths (about >8 ft) is affected little by seasonal temperature changes. Therefore, assuming a heat-generating waste that is more than several feet deep, there can be no stratification present in the headspace of any SST (an exception might be risers, but their volume is quite limited), so stratification effects will not be examined further.

(a) Antoniak ZI and KP Recknagle. 1996. *Modeling Tracer Gas Concentrations in Single-Shell Tank S-102 Dome.* TWSFG96.23, PNNL, Richland, Washington.

(b) Huckaby JL. Electronic communication (spreadsheet), July 8, 1996, PNNL.

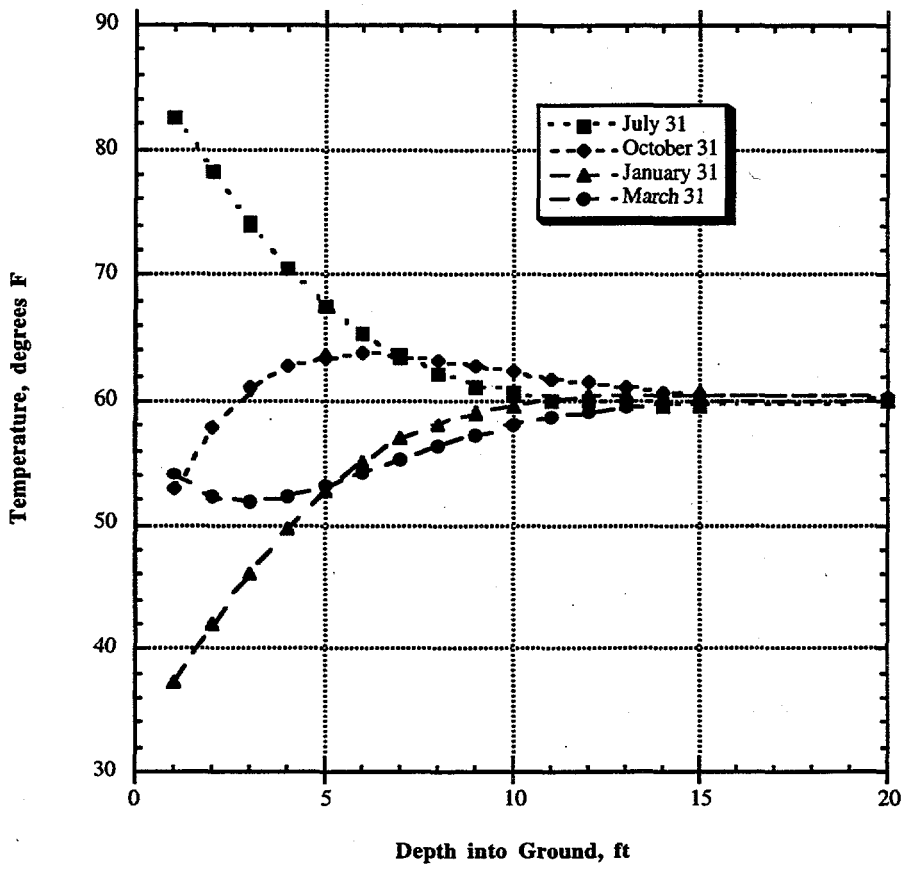

Figure 2.2. Hanford Subsoil Temperature Profiles as a Function of Season

2.2.3.2 Perturbation of Headspace Flow Field by Ventilation

It has been proposed that the air flow due to ventilation, or breathing, as it is called in passively ventilated tanks, might adversely affect the thermally driven convective flow field. We have simulated the thermally driven flow field in Tank S-102 both with and without the vent flow present to examine this issue.

Measured passive ventilation rates range from ~2 to ~20 cfm (Wilkins et al. 1997) with a median of about 5 cfm. This corresponds to a velocity of 1 ft/sec through a 4-in. vent line. Rapid barometric pressure changes can also produce high breathing rates for short periods. The fastest pressure change recorded for the Hanford Site was +0.50/-0.55 kPa/hr (+0.145/-0.160 in. Hg/hr) in 1958 (Stone et al. 1972). The flow through a 4-in. vent can be readily calculated for these conditions as about 10 cfm. The highest velocity in the vent would be less than 2 ft/sec.

A "chimney" effect has also been postulated to exist between adjacent, interconnected SSTs that differ appreciably in temperature. This could cause air from one tank to flow into the adjacent tank through the cascade overflow pipe. The typical range in temperature among SSTs in the same tank farm is about 10°C. The overflow lines connecting S-102 to adjacent SSTs S-101 and S-103

are 3-in. sched. 80 pipe located approximately 8 ft above the current waste level in S-102. Assuming a steady buoyancy-driven flow due to the full 10°C temperature difference through 10 m of this overflow line, the velocity is approximately 1 m/s (3 ft/sec) in the pipe for a flow rate of 8 cfm.

Based on these measurements and analyses, we chose an inlet velocity of 2 ft/s for the simulation as typical of passively breathing tanks. As discussed below, the result is essentially the same for much higher velocities in actively ventilated tanks.

The selected model simulated a plume-type of inflow of atmospheric air into the headspace of SST S-102 over a period of several hours. Inflow was assumed to occur at a velocity of 2 ft/sec solely through the 4-in.-diameter breather vent riser that is on a 9-ft radius from the tank center. Tank S-102 was chosen for this simulation because of the small-diameter vent and relatively small (65,000 ft^3 headspace); the high velocity associated with inflow through this small, single riser ought to have the greatest potential for creating significant local flow perturbations in the headspace. A different tank with a larger headspace (S-108, with 80,000 ft^3) was selected for the actual plume release simulations (see Section 4).

A 30-degree segment of Tank S-102 was modeled, with cells (in plan view–see Figure 2.3) only 2 degrees wide. A similar fine grid was selected in elevation (see Figure 2.4). The flow field was allowed to stabilize by running the simulation for two or more hours without the vent flow, and then vent flow was turned on and the simulation continued. In the plane of the vent there is little to distinguish between the pre- and post-vent flow fields (see Figures 2.5 and 2.6; the high velocity in Figure 2.6 is solely at the vent itself).

The flow field in both cases basically consists of a single huge Benard cell. In a vertical plane 4 degrees away from the vent there is also little evidence of significant perturbation caused by the vent flow (compare Figures 2.7 and 2.8). Two monitor cell locations, indicated by the boxed numbers 1 and 4 on Figures 2.7 and 2.8, were examined in greater detail by plotting the velocity components at those monitor cells. Comparing Figure 2.9 (with no vent flow) and Figure 2.10 (with the vent flow turned on for over two hours) shows negligible effects from the flow at monitor cell #1. The same holds true for Figures 2.11 and 2.12 at monitor cell #4. Therefore, we conclude that any vent flow caused by ambient pressure changes is highly unlikely to perturb the headspace flow field and thus will have negligible effect on hydrogen dispersion in the dome.

In the past, we also modeled plume dispersion in Tank SY-101, with forced ventilation flows ranging from 0 (vent flow shutdown) to 550 cfm (equivalent to 11.7 fps in our model), as well as intermediate values.[a] But directly under the vent and near it we found negligible differences among the calculated dome flow fields. Although we did not model these higher vent velocities in detail, it is highly unlikely that they would invalidate our conclusions, even for DSTs. A recent study on tank dome breathing in S-102 examined a vent inflow velocity of 4 fps and again found that the influence of this inflow rate is essentially confined to the vicinity of the vent and a small region below it.[b]

(a) Antoniak ZI and KP Recknagle. 1996. *Modeling Hydrogen Plume Concentrations in Single- and Double-Shell Tank Domes*. TWSFG96.12, PNNL, Richland, Washington.

(b) Antoniak ZI. July 10, 1996. *Modeling Breathing Effect on Gas Concentrations in a Single-Shell Tank Dome*. Letter report, PNNL, Richland, Washington.

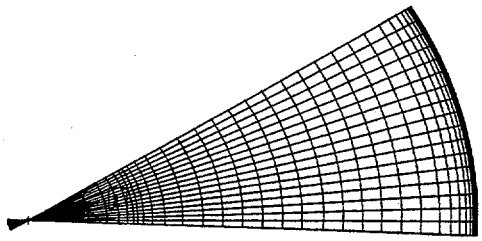

Figure 2.3. Plan View of Model

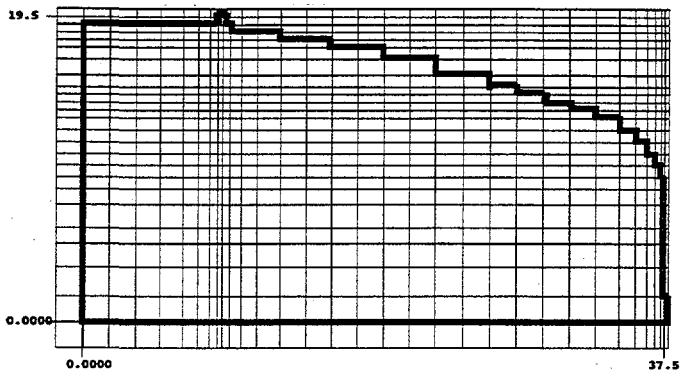

Figure 2.4. Elevation of Model

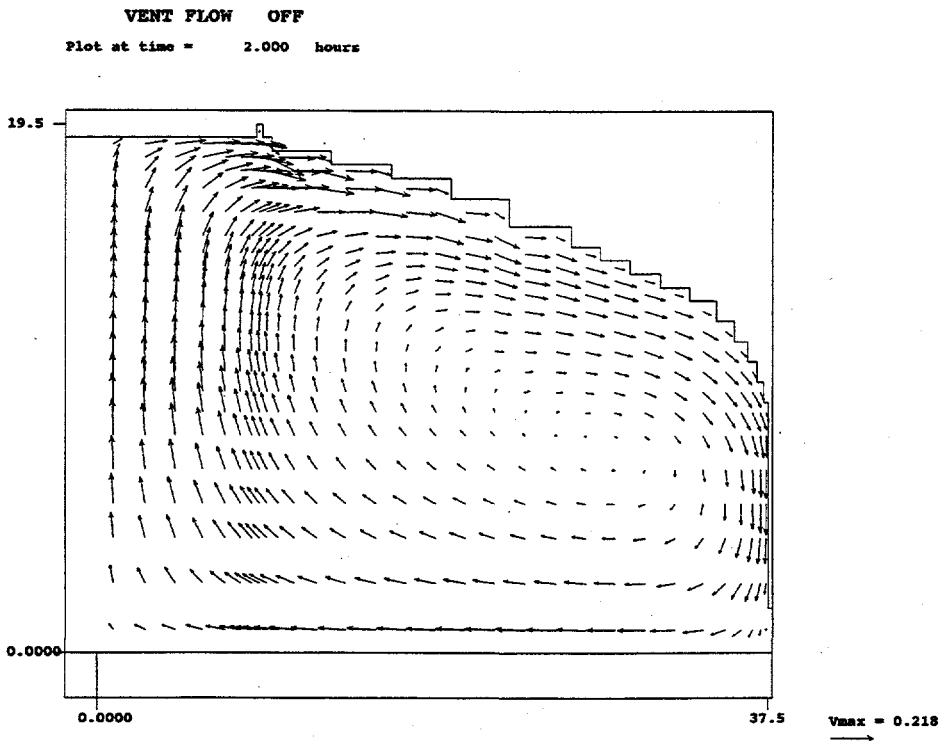

Figure 2.5. Flow Field Elevation at Vent with Vent off (end of 2-hr simulation)

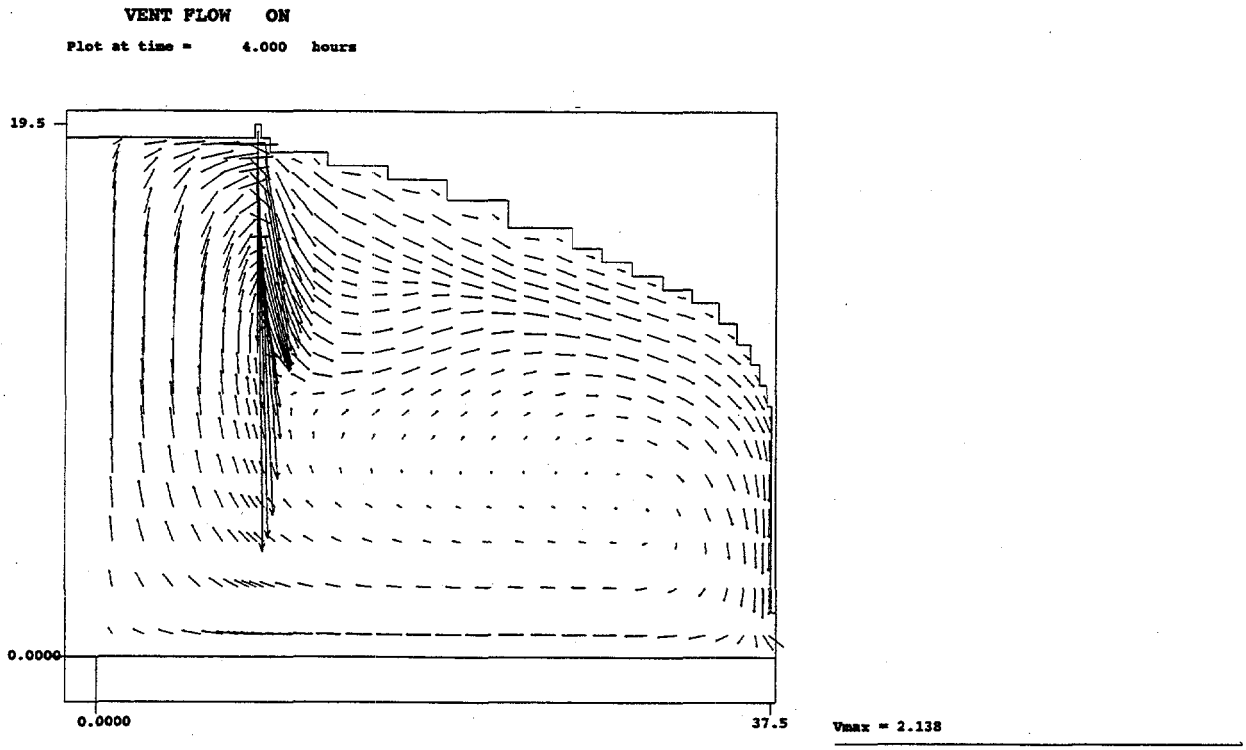

Figure 2.6. Flow Field Elevation at Vent with Vent on (end of 4-hr simulation)

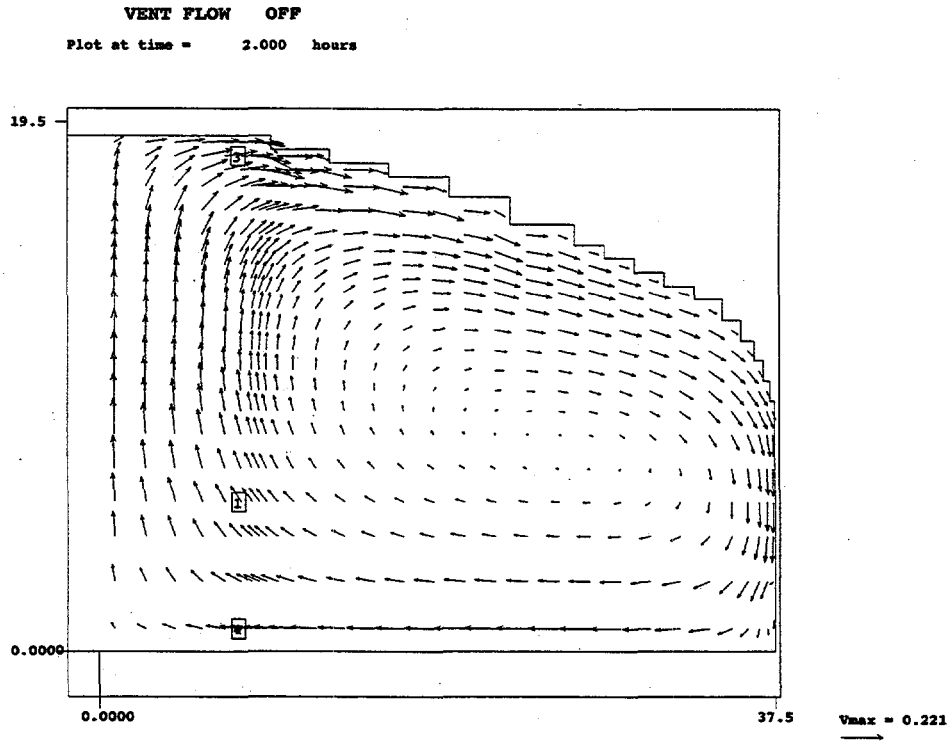

Figure 2.7. Flow Field Elevation near Vent with Vent off (end of 2-hr simulation)

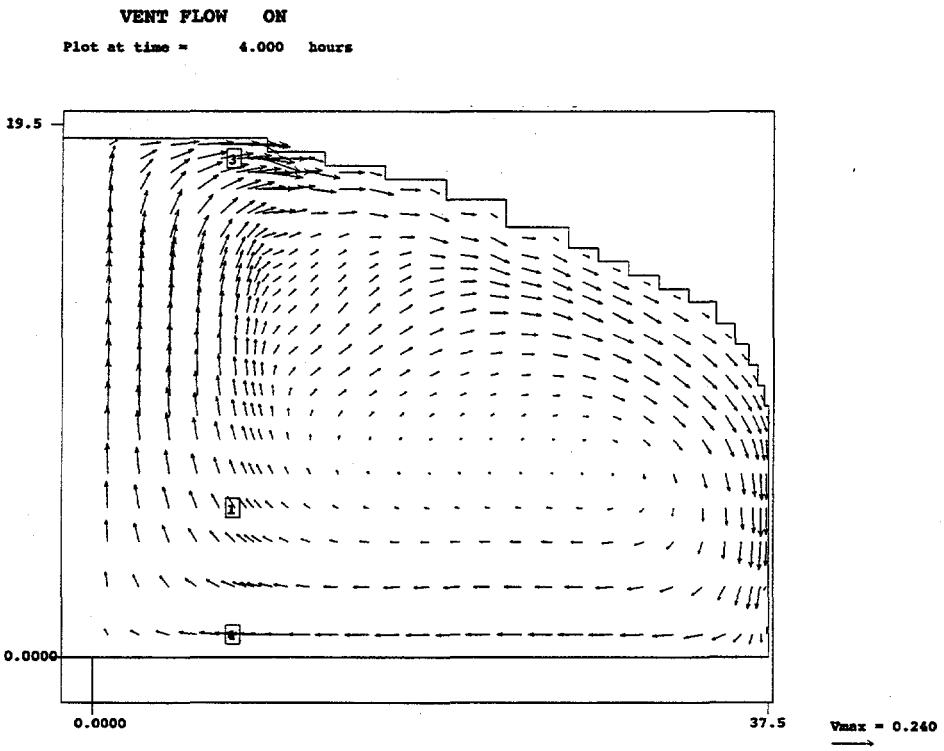

Figure 2.8. Flow Field Elevation near Vent with Vent on (end of 4-hr simulation)

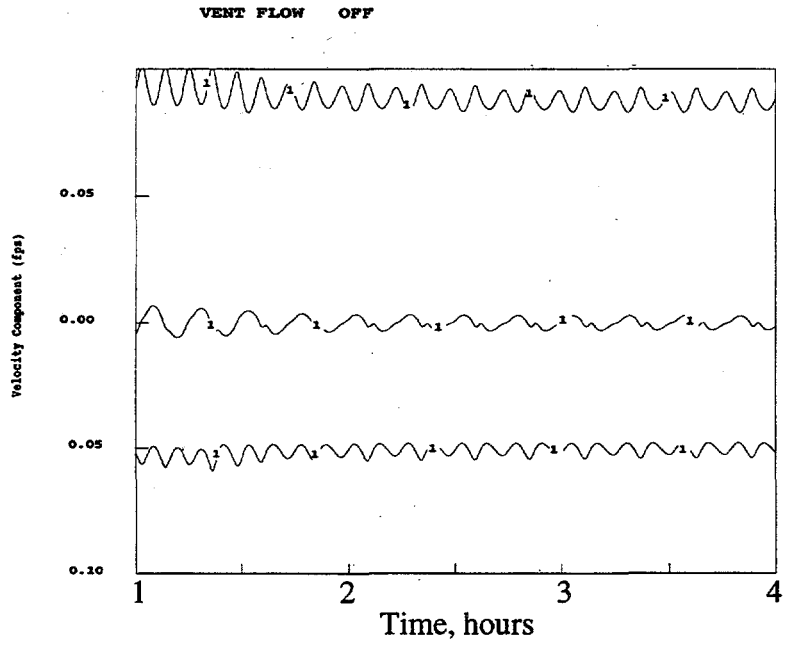

Figure 2.9. Velocity Components at Monitor Cell #1 (see Figure 2.7) with Vent off (from top, velocity components are V, vertical; W, circumferential; and U, radial)

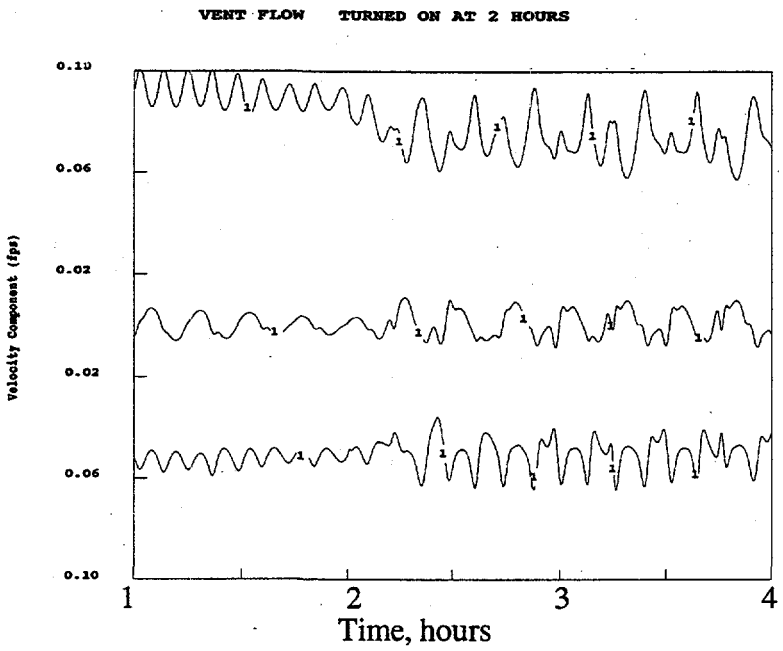

Figure 2.10. Velocity Components at Monitor Cell #1 (see Figure 2.7) with Vent on over 2 hr

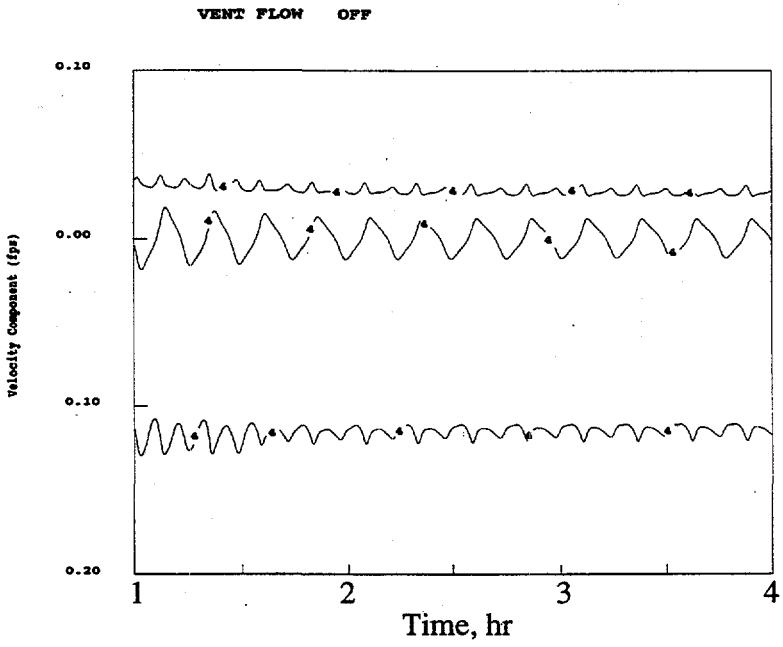

Figure 2.11. Velocity Components at Monitor Cell #4 (see Figure 2.7) with Vent off

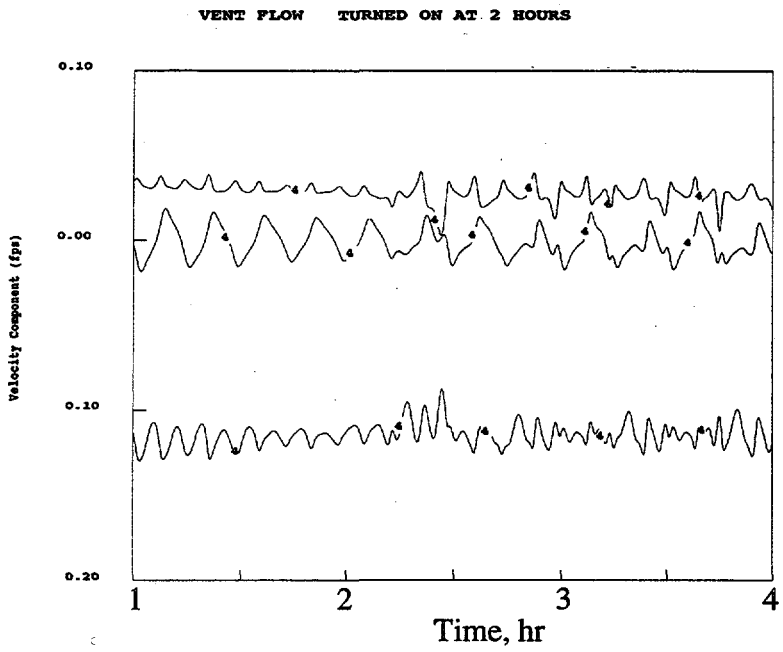

Figure 2.12. Velocity Components at Monitor Cell #4 (see Figure 2.7) with Vent on over 2 hr

In conclusion, all our studies to-date indicate that the flow field in a tank dome space, whether SST or DST, is dominated by natural convection. Forced flow breathing has only a localized influence on plume dispersion but has a long-term (i.e., hours) effect on the ultimate dilution of a plume. Recent gas concentration measurements in three SSTs show a homogenous dome atmosphere, indicating rapid mixing of any gases released from the waste by means of natural convection, even during conditions with minimal temperature gradients (Huckaby et al. 1997). Measurements of helium tracer gas concentrations in S-102 showed that the headspace was essentially fully mixed within an hour after gas injection[(a)] which agreed with pretest predictions of TEMPEST simulations.[(b)] Diffusion alone is too slow to account for these observations.

2.3 Other Parameters

A number of parameters have been determined to have a negligible effect after a cursory evaluation. The presence of structures (e.g. airlift circulators, saltwells) within the tank headspace should have a negligible effect on hydrogen dispersion, unless these structures occupy a large portion of the headspace volume. Evaporation, especially in SSTs, most of which have a fairly solid waste material with a limited amount of absorbed water, is expected to play only a very minor role in affecting dispersion. The major parameters discussed above and typical maximum ranges are summarized in Table 2.2 and evaluated in terms of the need for additional simulations.

(a) Huckaby JL. March 31, 1997. *Preliminary Report on Tank 241-S-102 Tracer Gas Testing.* Letter report TWSFG97.34, Pacific Northwest National Laboratory, Richland, Washington.

(b) Antoniak ZI and KP Recknagle. 1996. *Modeling Tracer Gas Concentrations in Single-Shell Tank 241-S-102 Dome.* Letter report TWSFG96.23, Pacific Northwest National Laboratory, Richland, Washington.

Table 2.2. Summary of Parameters and Ranges Considered

Parameter	Estimated (max/min = +/-)	How Determined	Determines/ Affects	Evaluation	Reference
Chimney effect	0.6 ft/sec (+)	intertank temp. diff.	dispersion	negligible	tank dome air temp. data
Hydrogen release volume	500 ft^3 (+)	TEMPEST, Safety Assess., history	concentration	consider	simulations
H_2 release duration	10 min. (-)	TEMPEST	concentration	consider	simulations
H_2 release location	near tank wall	TEMPEST	dispersion	consider[a]	(b)
H_2 release area	1 ft^2 (-)	TEMPEST cell	velocity	consider[a]	(b), (c, Fig. 8, 9)
H_2 release velocity[d]	6 ft/s (+)	TEMPEST	local concen.; mixing	consider[a]	(b), (c, Fig. 8, 9)
Ambient temperature	20-80°F[e]	meteorology; TEMPEST	dispersion	negligible[a]	(c, Fig. 11–13)
In-tank pipe/ obstruction	small area/ volume	estimate	-	negligible	-
Evaporation	very low rate	estimate	-	negligible	-

(a) Limited past simulations indicated a weak effect by this parameter.
(b) Antoniak ZI and KP Recknagle. 1996. *Modeling Hydrogen Plume Concentrations in a Single-Shell Tank Dome*. TWSFG96.6, PNNL.
(c) Antoniak ZI and KP Recknagle. 1995. *Modeling Post-GRE Spatial and Temporal Hydrogen Concentrations in Tank 241-101-AW Dome*. PNLFG:080295, PNNL.
(d) Not an independent parameter, but determines plume character.
(e) Because of the limited breathing by SSTs, only long-term (e.g., monthly average) temperatures are of interest.

3.0 Selected Parameter Ranges

The data in Table 3.1 are the actual parameters and ranges to be modeled for baseline transient plume studies. The logic used to construct the matrix was that the larger the release, the more likely it is to be faster and occur over a larger area. The release area, volume, and duration are the independent parameters. The release velocity and flow rates (shown in italics) are derived from these three. English units are used to be consistent with simulation output.

While individual cases were not tailored to match specific release mechanisms, the range of release volumes and durations was intended to cover the entire spectrum of sizes that might be considered. In general, the 10-minute releases represent DST GRE behavior. The 6,400 ft^3 corresponds to Event I, the last "rollover" that occurred in SY-101 before the mixer pump was installed (Meyer et al. 1997). This is about the largest release that might be called a plume because it was not quite large enough to bring the mixed headspace to flammability. A similar large, fast release might occur in DSTs as a result of a severe earthquake (Stewart et al. 1996; Reid and Deibler 1997). The 1,600 ft^3 release represents the few largest releases inferred from waste level history in Tanks AN-104 and AN-105. It might also represent the response of a typical SST to a severe earthquake. The 400 ft^3 release is typical of the historical gas release behavior of DSTs AN-103, AN-104, AN-105, and SY-103. The 100 ft^3 release might match a small gas release from a typical DST, though such GREs are too small to be detected in the waste level history.

The smallest, 100 ft^3, 100-minute release is what actually is being seen in the Standard Hydrogen Monitoring System (SHMS) data (Wilkins et al. 1997). Most of the observed releases actually occur over many hours; a ~2-hour release would be fast. The 400 ft^3, 100-minute release represents the behavior of DST AW-101 and the occasional slower release from some of the other DSTs. The 1,600- and 6,400-ft^3, 100-minute releases do not match any observed or postulated release profile but are included to provide a comparison with faster releases of the same volume.

Two additional simulations examine the influence of plume composition and plume buoyancy separately. The first increased the hydrogen concentration to 61.5% with carbon dioxide making up the balance to maintain the same buoyancy relative to air as the base case of 40% hydrogen and 60% air. In the second case the gas mixture was made negatively buoyant by using 40% hydrogen mixed with xenon and sulfur hexafluoride. This mixture is more than twice the density

Table 3.1. Summary of Selected Parameter Values for Baseline Simulations

Release area (ft^2)	*Exit velocity (ft/sec)*	*Release flow (ft^3/sec)*	Release volume (ft^3)	Release duration (min)	Rationale/tank for plume volume and duration parameter selection
1	*0.167*	*0.17*	100	10	hypothetical small DST release
4	***0.167***	***0.67***	**400**	**10**	typical DST historical release
16	*0.167*	*2.67*	1600	10	large DST historical or SST seismic
64	*0.167*	*10.67*	6400	10	SY-101 or large seismic release in DSTs
1	*0.0167*	*0.017*	100	100	larger SST release per SHMS data
4	*0.0167*	*0.067*	400	100	historic release in AW-101
16	*0.0167*	*0.267*	1600	100	hypothetical large, slow release
64	*0.0167*	*1.067*	6400	100	hypothetical large, slow release

of the heaviest in-situ gas mixture measured with the RGS so far, which is only slightly negatively buoyant.[a] The appropriate parameters are listed in Table 3.2, where they are compared with the base case, which is listed in boldface type in Table 3.1.[b]

The last simulations to be done modeled a continuous, steady-state release of 25 cfm of hydrogen/air, in the 40/60% mixture used in Table 3.1 base cases, for two assumed breathing rates that are chosen roughly to cover the range of measured and/or calculated SST breathing rates (Johnson et al. 1997, pp. 4-17–4-18). Data for those simulations are given in Table 3.3. These last runs bring the total number of small plume simulations to 12.

Table 3.2. Simulations That Vary Plume Composition and Buoyancy

Simulation	H_2 (%)	Other gases		Molecular weight	ρ_{MIX}/ρ_{AIR}
		(%)	Species		
Base case (Table 3.1)	40	60	air	18.18	0.63
High H_2	61.5	38.5	CO_2	18.17	0.63
Negative buoyancy	40	60	Xe; SF_6	79.40	2.74

Table 3.3. Steady-State Release Simulations

Area (ft^2)	Velocity (ft/s)	Release flow rate			Vent flow cfm	Mixed H_2 concentration[a]
		(ft^3/s)	(cfm)	(ft^3/day)		
~1	$2.4(10^{-4})$	2.9E-04	0.017	25	5.6[b]	0.12%
~1	$2.4(10^{-4})$	2.9E-04	0.017	25	0.56[c]	1.2%

(a) At fully mixed and diluted (i.e., asymptotic) conditions.
(b) Assumes 10% of S-108 dome air is exchanged daily (Johnson et al. 1997, pp. 4-17–4-18), approximating the mean passive vent rate in SSTs.
(c) Assumes 1% of S-108 dome air is exchanged daily, approximating pressure breathing only.

(a) The gas in the wet saltcake layer in U-103 had 31% nitrogen, 14% hydrogen, and 52% nitrous oxide, as reported in PNNL letter report TWSFG97.40, May 1997.
(b) The other gases were selected strictly for convenience in modeling. As long as the mixture density is correct, the actual species are immaterial to the calculation. The properties of the gases used happen to be installed in the TEMPEST code.

4.0 Simulations

4.1 Approach

The objective of the present work was to model the hydrogen gas concentrations that result from a plume-type release in an SST with an established buoyancy-driven flow pattern . The steady-state velocity field was established by running a 60-minute simulation prior to plume release. The simulations were run with the TEMPEST code using a previously developed Tank S-108 model.[a] The plume release point was assumed to be near the tank wall, and the outlet for the dome air was placed diametrically opposite and low in the dome. Outflow is only continuitive; no inlet ventilation flow is provided. These assumptions are conservative. The k-ε turbulence model available in TEMPEST was purposely inactivated. However, molecular diffusion of gas species is allowed.

4.1.1 TEMPEST Model

Figure 4.1 represents a plan view of the computational model and shows the release points and vent location. Figure 4.2 gives an elevation of the model at the vent and shows that the vent is at the dome crest. The computational model contained 33 radial cells, 22 vertical cells, and 27 azimuthal cells. One or more cells on the surface were used as the gas plume source. The hydrogen/air gas mixture was released from the variable-area source cells with an initial upward velocity as specified in Table 3.1. The local density of the gas mixture is computed from its composition and temperature.

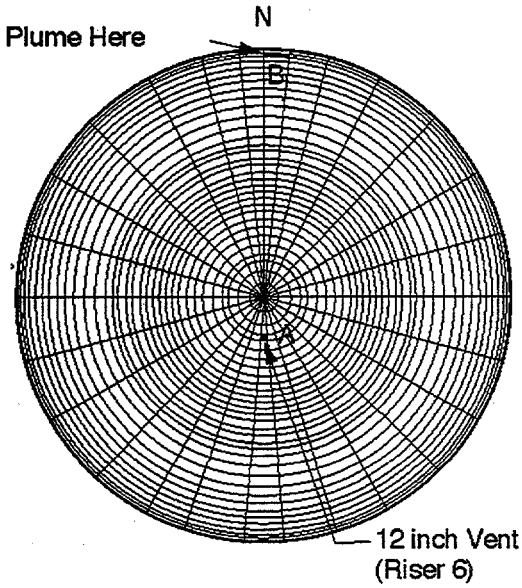

Figure 4.1. Plan View of S-108 Model Domain

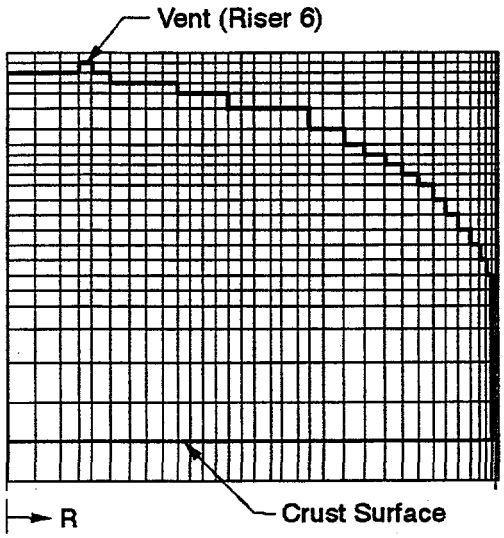

Figure 4.2. Elevation of S-108 Model in the Vent Plane

(a) Antoniak ZI and KP Recknagle. 1996. *Modeling Hydrogen Plume Concentrations in a Single-Shell Tank Dome*. TWSFG96.6, PNNL, Richland, Washington.

The model included heat transfer by convection and conduction from the waste surface to the gas and from the gas to the dome. Both the waste surface and dome walls were isothermal with the waste 2°F warmer than the walls. The same model was used for both validation and plume parametric runs; however, for conservatism, we elected to inactivate the turbulence model in TEMPEST for the actual plume dispersion simulations. However, TEMPEST simulations with the turbulence model turned off cannot really be classed as "laminar." Entrainment by momentum exchange is still included even without a turbulence model.

4.1.2 Model Validation

The TEMPEST code has been validated previously for plume studies (Meyer and Fort 1993; Eyler et al. 1983). Validation testing has included the modeling of hydrogen transport in reactor containment structures under a variety of conditions, resulting in good agreement with experimental data (Trent and Eyler 1985). Because hydrogen transport in the waste tank dome space is such an important issue, further validation was performed under the Flammable Gas Program in FY 1996 with parameters selected to represent tank conditions. The results of this work is reported in this section.

The experimental and analytical study of buoyant jets in Abraham (1963) provides relevant data with which to compare TEMPEST results. Although Abraham used water in his experiments, a comparison is valid for gases as well because the (turbulent) Schmidt numbers for water and gases are equal (~1). Therefore, the diffusivity of momentum versus the diffusivity of mass are correctly matched for the materials discussed.

The TEMPEST k-ε model was used to obtain the effective turbulent viscosity (Trent and Eyler 1991) for these tests. The k-ε model is perhaps the one most frequently used (Anderson et al. 1984). The closure relations of this model have been found to compare reasonably with experimental data for an axisymmetric (purely) buoyant plume, except for underprediction of axial turbulent transport (Shabbir and Taulbee 1990).

Validation was performed using Abraham's (1963) data taken at a Froude number of 5 because more data were taken there. The Froude number (F) is defined as the ratio between inertial and gravity forces = $\rho U^2/D/\rho g$, and provides a means for evaluating the relative importance of jet exit velocity versus buoyancy in determining the jet structure. A modified, so-called densimetric Froude number is used in the literature and defined as

$$F = (\rho_o U^2/D)/(\rho_s - \rho_o)g$$

where U is the plume exit velocity, D is the exit diameter, ρ_s is the density of the dome air, and ρ_o is the density of the (hydrogen-containing) gas released.

Pure hydrogen plumes of fairly high velocity (>25 ft/sec) approach a Froude number ~1. The main reason for the low Froude numbers of plume releases is the large density difference between air and a plume of 100% hydrogen. Such a plume is clearly buoyancy-dominated even at a high exit velocity from the waste. Plumes that have, in addition to hydrogen, a significant amount of denser gas attain F >1 at considerably lower velocities. Therefore, for releases of a mixture of gases ejected from a relatively small area (~1 ft diameter), it is reasonable to assume that F numbers in the range of 1 to 5 are possible. This would also hold true for larger mixed-gas releases in DSTs, even though these would be ejected through larger areas.

As shown in Figure 4.3, our validation study encompassed two Re_D numbers and several different potential core grids. The first four TEMPEST plots are for a heated air plume with Re_D = 1600 and with a varying number potential core cells, as identified in the legend. For example, the

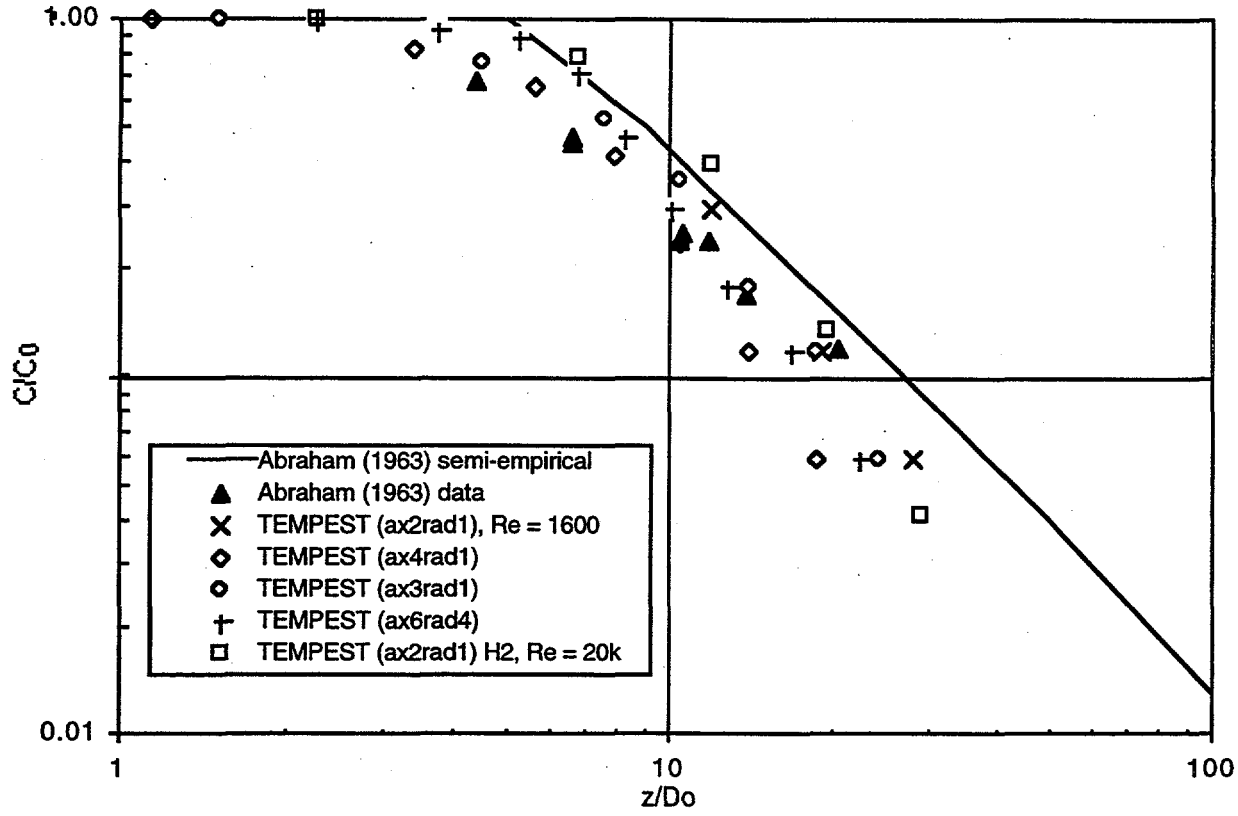

Figure 4.3. Comparison of TEMPEST Results with Abraham (1963) for F = 5

first result, identified as "ax2rad1," signifies a potential core grid structure consisting of one radial and two axial cells. Reasonably good agreement with the data and semi-empirical correlation is obtained with a simple cell structure in the core; this noding was also used for the last run, with a hydrogen release at $Re_D = 20{,}000$, and good agreement was again obtained.

The N33.5f version of TEMPEST was used to obtain the results shown in Figure 4.3; we also exercised the T2 version, including the option of defining the gases as thermally expanding. The default (nonthermally expanding) option in both N33.5f and T2 employs the well-known Boussinesq approximation that treats the gas density as constant in all the governing equations except for the body force terms of the momentum equations. The T2 results were nearly identical to the N33.5f results and are not shown here.

4.2 Numerical Diffusion

Truncation error that is present in a finite difference code such as TEMPEST introduces an artificial diffusion into the solution (Anderson et al. 1984, p. 92) that is often called numerical diffusion. This error tends to reduce all gradients and would therefore tend to indicate more rapid mixing than actually occurs in the simulations discussed above. The magnitude of this error, especially for a fully three-dimensional simulation, is difficult to estimate (Roache 1976, p. 66).

We examined this issue by calculating a one-dimensional artificial viscosity (Roach 1976) evaluated at conditions typical of a TEMPEST plume simulation such as cell size, velocity, and time step. This viscosity term equals about 0.18 ft^2/sec (for a Schmidt number ~1, typical of

gases, this would also represent the value of the gas diffusivity); the actual diffusivity of hydrogen in air is ~6.6E–4 ft^2/sec. This large viscosity term was derived based on an upwind finite difference scheme, which is only first-order accurate (Roache 1976, p. 64), while TEMPEST uses the Crank-Nicholson differencing scheme that has the potential of being second-order accurate (Anderson et al. 1984, p. 405). We then modified the value of the hydrogen diffusivity to this much larger value and reran one of the above simulations. Comparing the two runs made with these two diffusivities showed essentially imperceptible concentration differences because convection is a much more powerful agent for dispersion than diffusion. Therefore, we conclude that the presence of numerical diffusion in TEMPEST is not an important factor for the class of problems we have simulated.

4.3 Plume Simulation Results

The results of all the simulations are summarized in Table 4.1. It is clear that only the largest plumes present a significant flammability hazard. Except for the largest (6,400 ft^3), fastest (10-minute) plume, flammable conditions exist only during the actual release. Long (100-minute) releases (again, except for the 6,400 ft^3 plume) never become flammable within the resolution of the model. That is, it is possible that a small region (containing less than 12 ft^3 hydrogen for the 1,600 ft^3 release, and proportionately less for the smaller plumes) exists right at the plume exit from the waste but is not resolved by our present model that has typical cell volumes of 2 ft^3. These results are consistent with our earlier modeling activities and with tracer gas experiments.[a]

Table 4.1. Summary Results of Simulations[a]

Release area (ft^2)	Release velocity, (ft/sec)	Release volume (ft^3)	Release duration (min)	Plume flammability		Fig. #/Comment (also see notes)
				max. vol. (ft^3)[b]	duration (min)	
0.99	0.169	100	10	4	10	Fig. 4.6 and 4.7
4.39	0.152	400	10	28	10	-
4.39	0.152	400	10	52	10	0.62 H_2/0.38 CO_2
4.39	0.152	400	10	~0	-	0.60 Xe or SF_6[c]
14.55	0.183	1,600	10	141	10	Fig. 4.8 and 4.9
67.88	0.157	6,400	10	32,000[d]	133	Fig. 4.4; 4.10–4.13
0.99	0.017	100	100	~0	-	-
4.39	0.015	400	100	~0	-	-
14.55	0.018	1,600	100	~0	-	-
67.88	0.016	6,400	100	95	10	Fig. 4.5
0.99	0.00024	-	-	0	-	Steady state, nom. vent
0.99	0.00024	-	-	0	-	Steady state, low vent

(a) All simulations used 60% air/40% hydrogen unless stated otherwise (two cases).
(b) A maximum volume flammable of ~0 implies that any flammability is confined strictly to the release cells at most.
(c) Both Xe and SF_6 simulations were run; there was no significant difference in results.
(d) The flammable volume, with a hydrogen concentration ≥4%, can exceed the original plume volume that contained 40% hydrogen by volume by up to a factor of 10.

(a) Huckaby JL. July 23, 1997. Private communication (spreadsheet). PNNL, Richland, Washington.

The flammability behavior of the 10- and 100-minute, 6,400 ft^3 plumes is provided in Figures 4.4 and 4.5, respectively. Note that the peak flammable volume of 32,000 ft^3 is exactly half of the 64,000 ft^3 that could potentially be made flammable by a 6,400 ft^3 release of a mixture consisting of 40% hydrogen. The peak 95 ft^3 flammable volume in the 100-minute release is an insignificant fraction of the potential flammability.

Additional insight is provided by Figures 4.6–4.13, which illustrate the progressive stages of plume release and evolution. The figure captions contain information on the plume volume/ release area/release duration. The smallest release modeled (100 ft^3 over 10 minutes) is shown in Figures 4.6 and 4.7; the hydrogen concentrations present in the dome at the end of the release period are shown in Figure 4.6, with essentially no flammable volume present. A short time later concentration gradients are significantly lower, as shown in Figure 4.7. Note that the maximum contour color represents a hydrogen concentration of only 1%. Note also that the colors and contours near the left and bottom borders of the plots are artifacts of the plotting programs and should be ignored.

The progression of a significantly larger plume release of 1,600 ft^3 in 10 minutes is similarly illustrated by Figures 4.8 and 4.9. Note that the color range is expanded now, with the maximum contour color (a very light pink, or salmon) now representing the LFL concentration of hydrogen, or 4%. From Figure 4.8 it is clear that a flammable concentration exists but is essentially confined to the plume itself. An hour after the release ends, only concentrations well below the LFL are present, as shown in Figure 4.9.

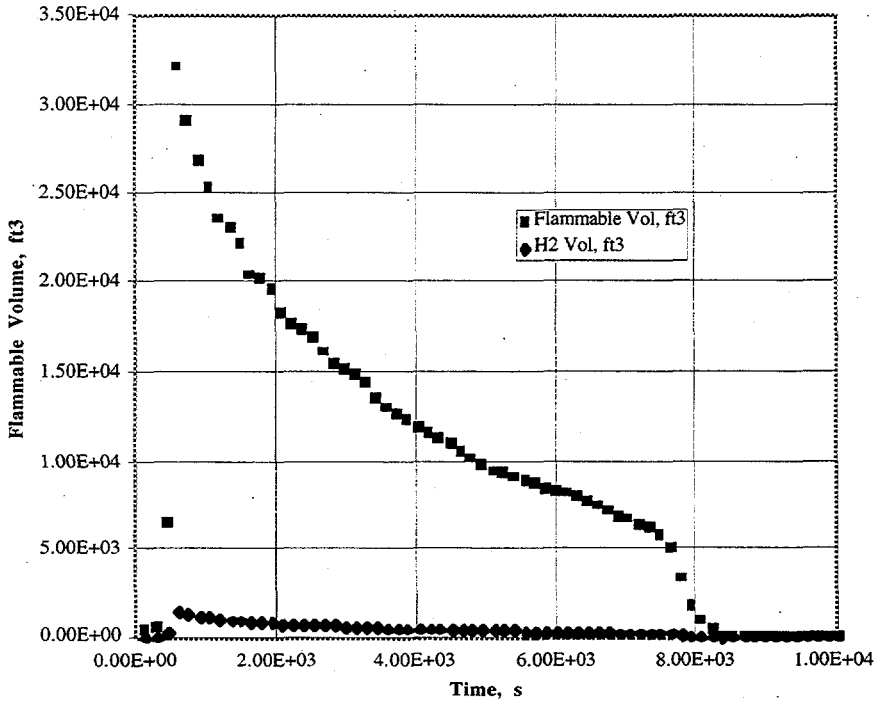

Figure 4.4. 6400-ft^3 Plume Released over 10 Minutes Through 64 ft^2

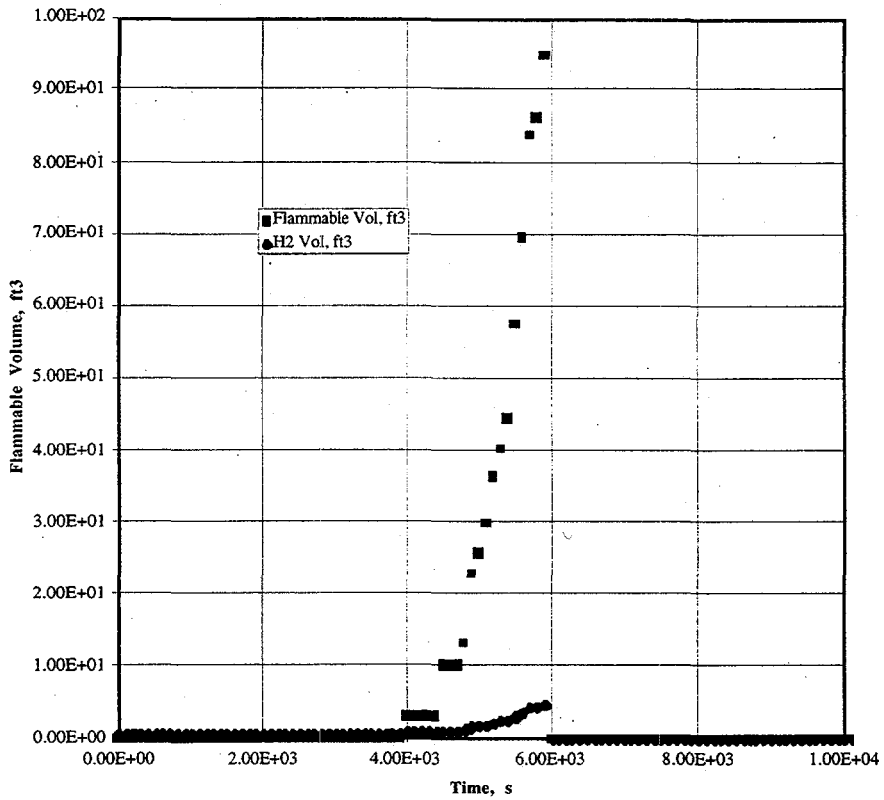

Figure 4.5. 6400-ft^3 Plume Released over 100 Minutes Through 64 ft^2

As one might expect, the largest release modeled, 6,400 ft^3 in 10 minutes, provides the most interesting dispersion plots, shown in Figures 4.10–13. The contour color range used here is the same as in Figures 4.8 and 4.9. A small flammable volume is present shortly after the plume begins in Figure 4.10 and expands to include a large portion of the entire dome volume by the end of the 10-minute release period in Figure 4.11. Figure 4.12 shows that, even an hour after the release ends, a large percentage of the dome volume remains above LFL concentration . But after another two hours, all hydrogen concentrations are below the LFL, as shown in Figure 4.13.

The effect of increasing the hydrogen concentration is to provide more potentially flammable volume. However, since the flammability threshold is fixed at the LFL, a higher hydrogen concentration has a stronger effect than the ratio of concentrations would indicate. The case of a 400 ft^3 release with 62% hydrogen created about twice the flammable volume as the same case with 40% hydrogen; increasing hydrogen by a factor of 1.5 increased the flammable volume by a factor of 2. However, it must be remembered that, in both cases, the flammable volume was only ~1% of the potential flammable volume.

Only one additional case tested the effect of negative buoyancy, so no firm conclusions can be drawn. The 400 ft^3 release with 60% xenon (or SF_6) did not create a flammable volume within the precision of the descretization compared with a ~1% flammability with the mildly buoyant base case. Neutral buoyancy, which was not investigated, is the more likely case for actual waste gas.

The continuous background (steady state) release does not create a stratified layer with flammable concentrations of hydrogen, even with extremely low ventilation. The potential for local stratification in dead-end risers was not investigated.

Figure 4.6. Plume = 100 ft3/1ft2/10 minutes
(At end of 10 minute release)

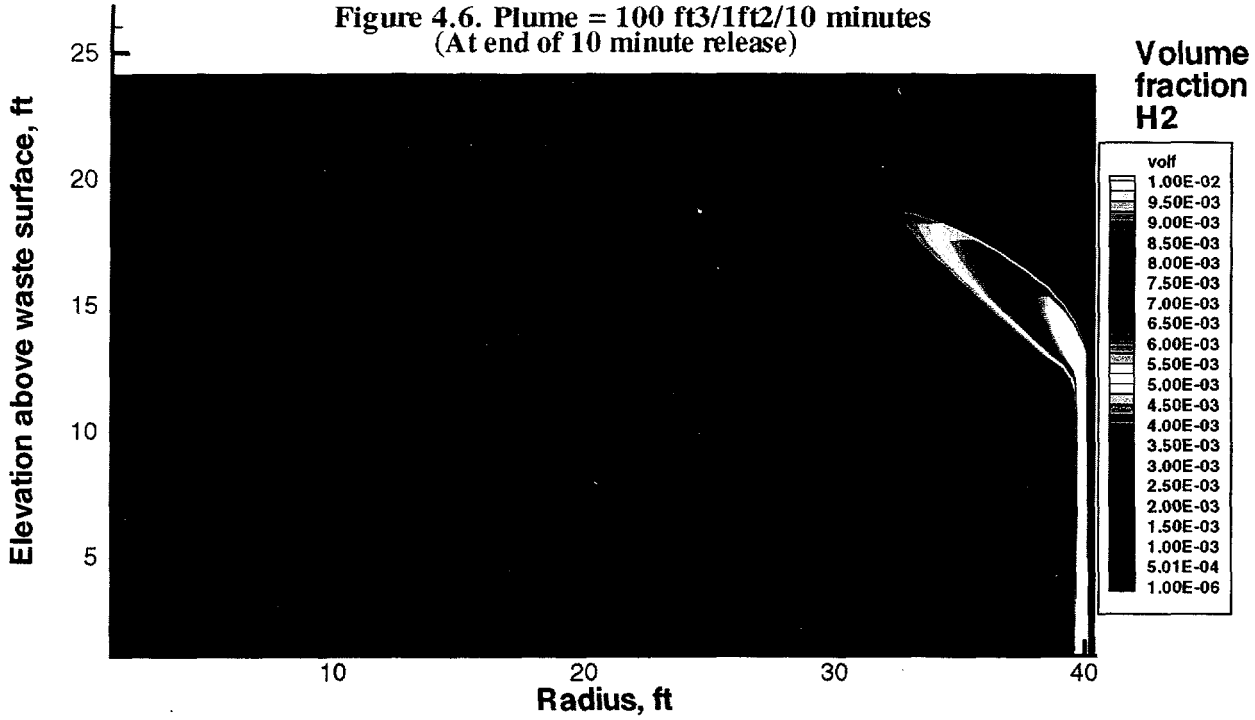

Figure 4.7. Plume = 100 ft3/1ft2/10 minutes
(10 minutes after release ends)

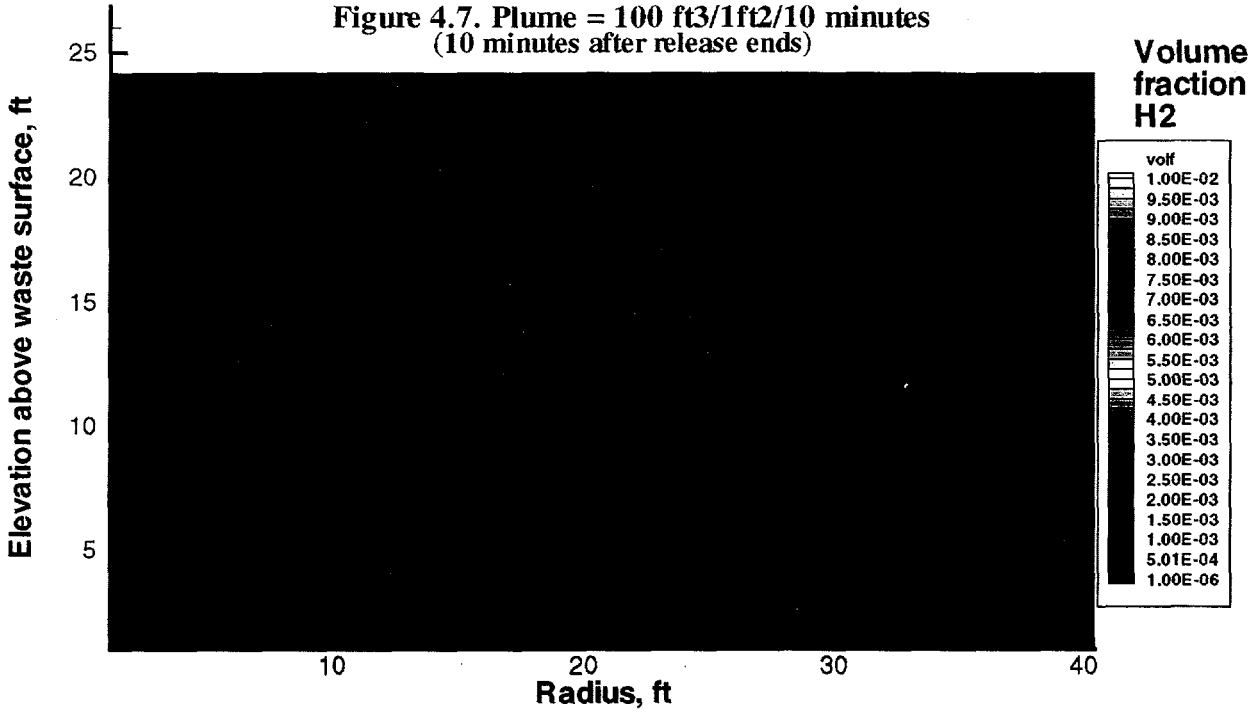

Figure 4.8. Plume = 1600 ft3/16ft2/10 minutes
(At end of 10 minute release)

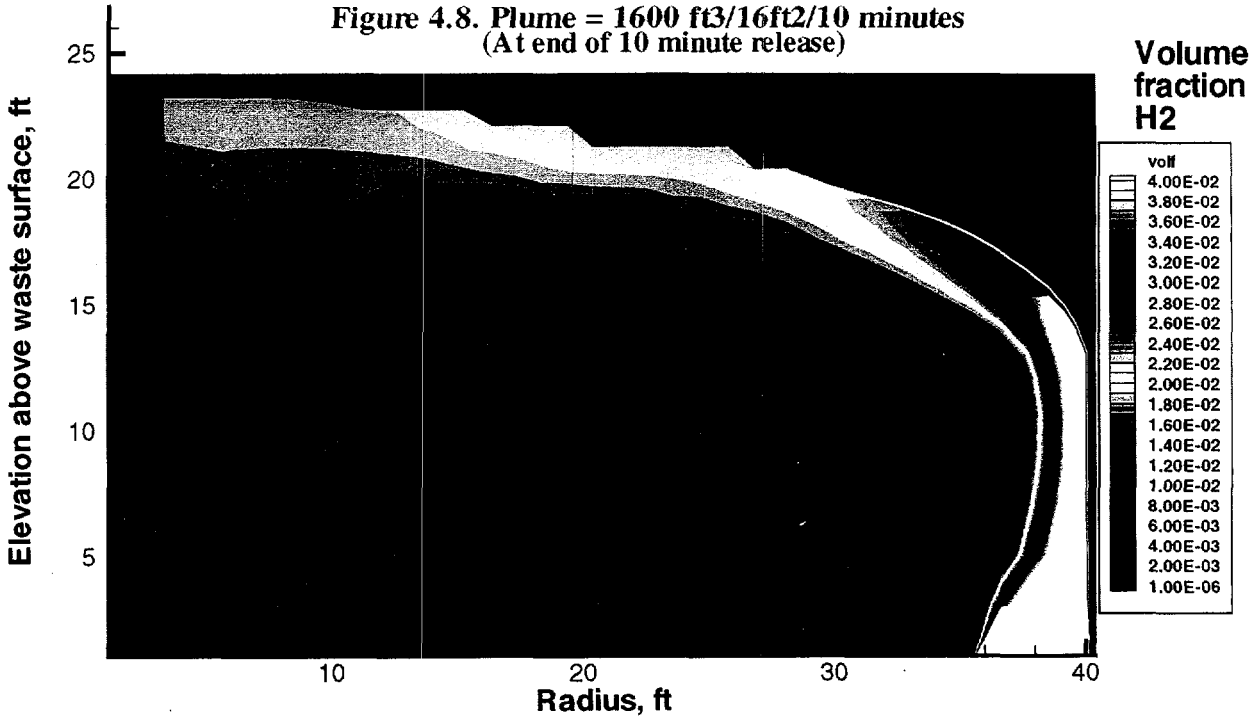

Figure 4.9. Plume = 1600 ft3/16ft2/10 minutes
(1 Hour after release ends)

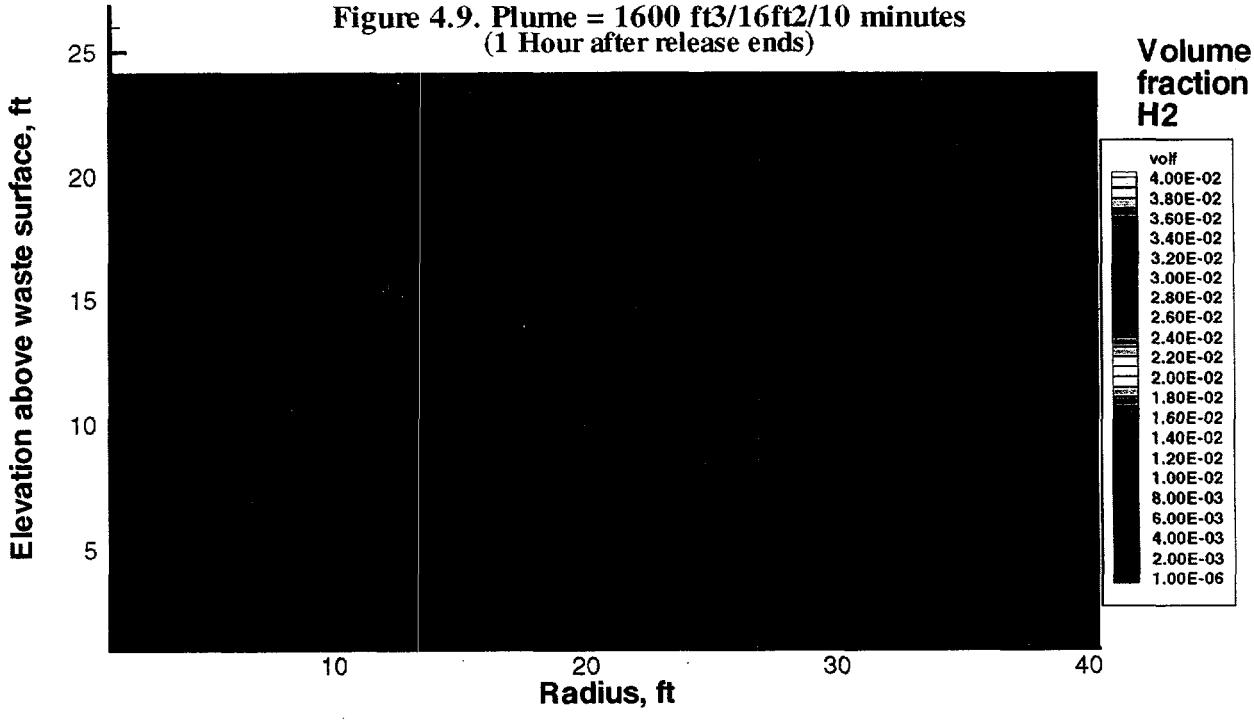

Figure 4.10. Plume = 6400 ft3/64ft2/10 minutes
(After 2.5 minutes of release)

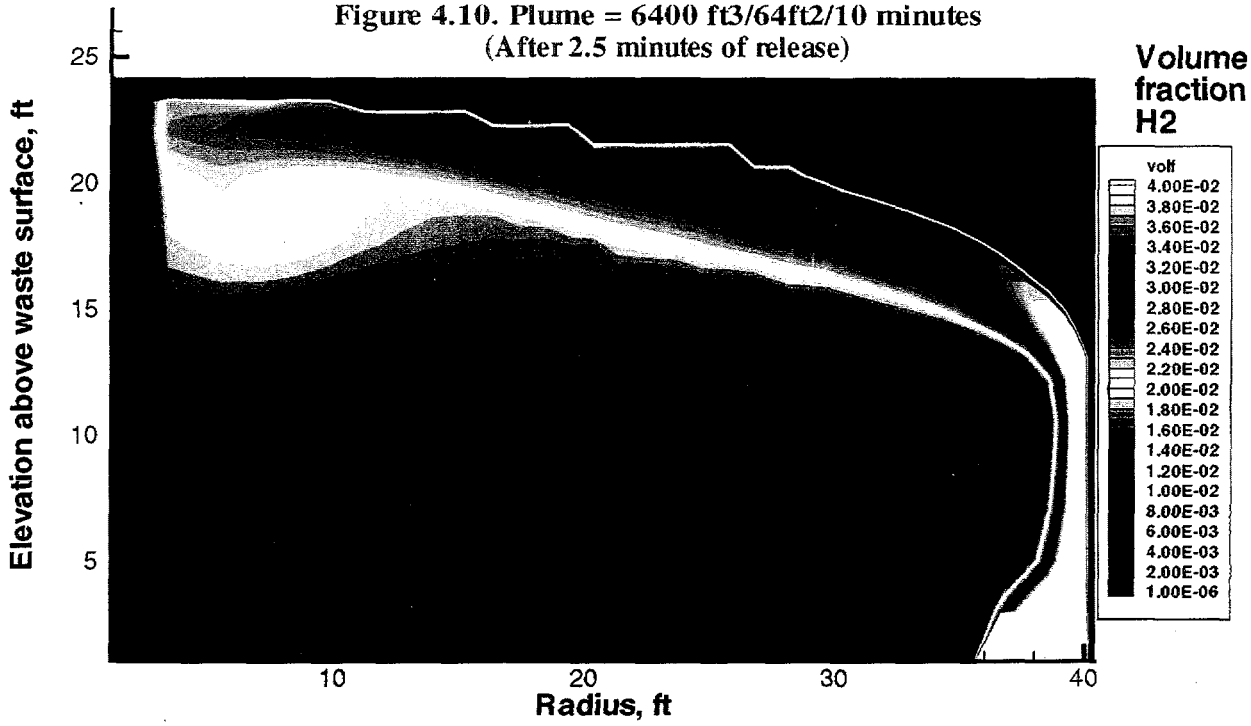

Figure 4.11. Plume = 6400 ft3/64ft2/10 minutes
(At end of 10 minute release)

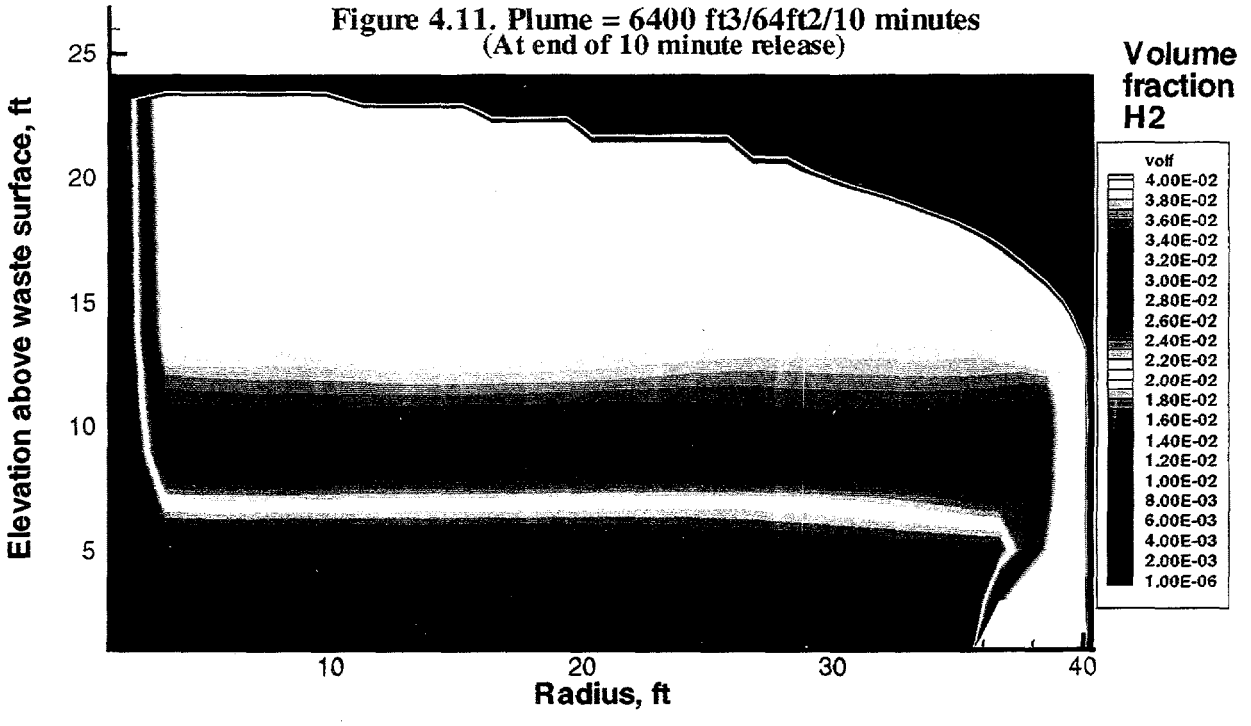

Figure 4.12. Plume = 6400 ft3/64ft2/10 minutes
(1 hour after release ends)

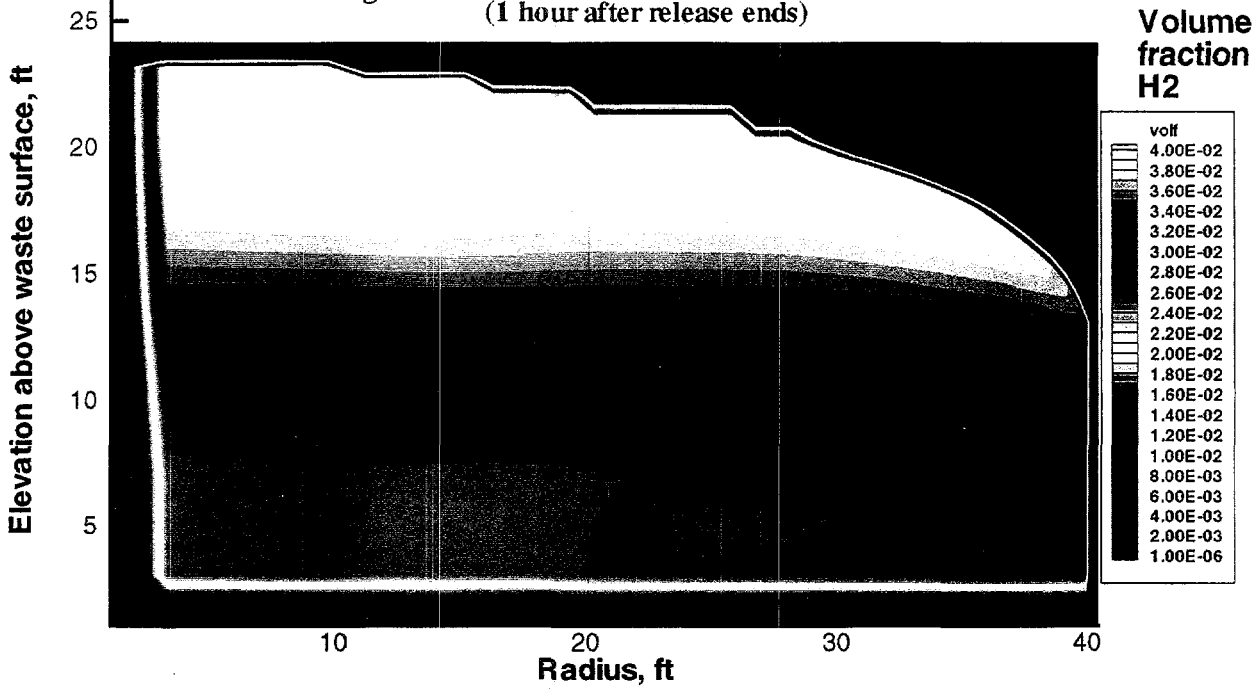

Figure 4.13. Plume = 6400 ft3/64ft2/10 minutes
(3 hours after release ends)

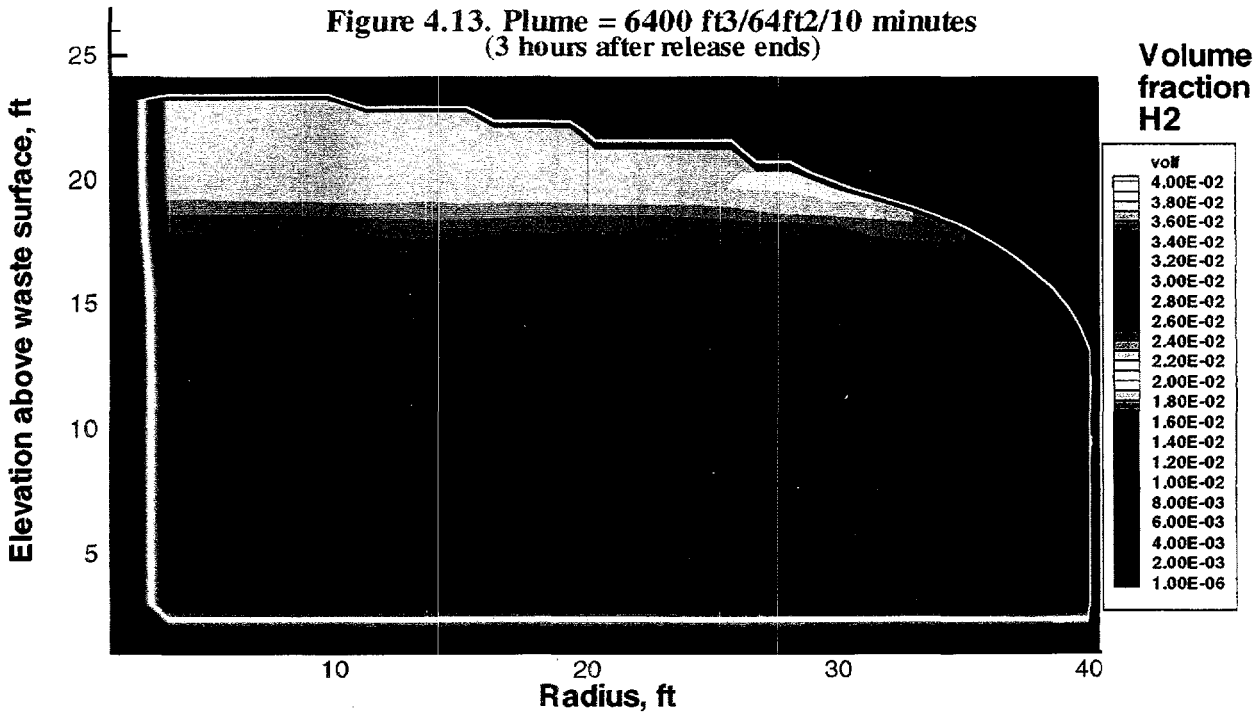

4.4 Conclusions and Recommendations

Twelve plume release simulations were run that encompassed a broad range of plume configurations and sizes. The results indicate that all flammable gas plume-type releases that fall within historical volume ranges will remain flammable only during the actual release itself, and the actual flammable volume will comprise only a small fraction of the total hydrogen volume released in the plume. Mixing in tank dome spaces is so rapid that, as soon as the release ends, so does the potential for a locally flammable concentration. Only for very large releases of many thousands of cubic feet, which would raise the mixed headspace concentration to a significant fraction of the LFL, can flammable gas concentrations persist for several hours after the release ends.

Though these results are significant, some additional effort is needed to close the issue of plume release flammability. The issue of buoyancy needs to be investigated in more detail, emphasizing approximate neutral buoyancy rather than negatively buoyant (with respect to air) gas mixtures. Additional plume simulations need to be run with release volumes set between the two largest ones studied here (1,600 and 6,400 ft^3) to better define the point at which the flammable volume becomes significant. Finally, while we believe it is clear that passive ventilation flow does not affect plume dispersion, the effect of high, active ventilation flow on flammability time needs to be evaluated for some larger releases.

5.0 References

Abraham G. 1963. *Jet Diffusion in Stagnant Ambient Fluid.* Ph. D. dissertation at the Technological University, Delft, Holland (Pub. No. 29 of Delft Hydraulics Laboratory).

Allemann RT, ZI Antoniak, WD Chvala, LE Efferding, JG Fadeff, JR Friley, WB Gregory, JD Hudson, JJ Irwin, NW Kirch, TE Michener, FE Panisko, CW Stewart, and BM. Wise. 1994. *Mitigation of Tank 241-SY-101 by Pump Mixing: Results of Testing Phases A and B.* PNL-9423, Pacific Northwest National Laboratory, Richland, Washington.

Anderson DA, JC Tannehill, and RH Pletcher. 1984. *Computational Fluid Mechanics and Heat Transfer.* Hemisphere Publishing Corp., New York, p. 222.

Anderson DA, JC Tannehill, and RH Pletcher. 1984. *Computational Fluid Mechanics and Heat Transfer.* Hemisphere Publishing Corporation, Washington, DC.

Brown RG and R Stout. 1996. *Compilation of Hydrogen Data for 22 Single-Shell Flammable Gas Watch List Tanks.* WHC-SD-WM-ER-576 Rev. 0, Westinghouse Hanford Company, Richland, Washington.

Cussler EL. 1984. *Diffusion: Mass tranfer in fluid systems.* Cambridge University Press, Cambridge, GB.

Eyler LL, DS Trent, and MJ Budden. 1983. *TEMPEST: A Three-Dimensional Time-Dependent Computer Program for Hydrothermal Analysis, Vol II: Assessment and Verification Results.* PNL-4348 Vol. II, Pacific Northwest National Laboratory, Richland, Washington.

Eyler LL and DS Trent. 1982. *Computation of Hydrogen Gas Distribution Using TEMPEST Computer Code: Standard Problem Blind Calculation Results.* FATE-82-101, Pacific Northwest National Laboratory, Richland, Washington.

Fric TF and A Roshko. 1994. "Vortical Structure in the Wake of a Transverse Jet." *J. Fluid Mech*, v. 279, pp. 1–47.

Hodgson KM. 1996. *Evaluation of Hanford Tanks for Trapped Gas* WHC-SD-WM-ER-526, Westinghouse Hanford Company, Richland, Washington.

Huckaby JL, L Jensen, RD Cromar, SR Wilmarth, JC Hayes, LL Buckley, and LD Pennington. 1997. *Homogeneity of Passively Ventilated Waste Tanks.* PNNL-11640, Pacific Northwest National Laboratory, Richland, Washington.

Johnson GD, WB Barton, JW Brothers, SA Bryan, PA Gauglitz, RC Hill, LR Pederson, CW Stewart, and LM Stock. 1997. *Flammable Gas Project Topical Report.* HNF-SP-1193 Rev. 2, Richland, Washington.

Kulkarni AK, F Murphy, and SS Manohar. 1993. "Interaction of Buoyant Plumes with Two-Layer Stably Stratified Media." Experimental Thermal and Fluid Science, v. 7, pp. 241–248

LANL. 1996 *A Safety Assessment for Salt Well Jet Pumping Operations in Tank 241-A-101: Hanford Site, Richland, Washington.* WHC-SD-WM-SAD-036 Rev. 0, prepared by Los Alamos National Laboratory for Westinghouse Hanford Company, Richland, Washington.

Meyer PA and JA Fort. 1993. *TEMPEST: A Computer Program for Three-Dimensional Time-Dependent Computational Fluid Dynamics, Vol. 3: Validation and Verification.* PNL-8857 Vol. 3 Rev. 0, Pacific Northwest National Laboratory, Richland, Washington.

Popiel CO and O Trass. 1991. "Visualization of a Free and Impinging Round Jet." *Experimental Thermal and Fluid Science*, v. 4, pp. 253–264.

Roache PJ. 1976. *Computational Fluid Dynamics.* Hermosa Publishers, Albuquerque, New Mexico.

Shabbir A and DB Taulbee. 1990. "Evaluation of Turbulence Models for Predicting Buoyant Flows." *J. Heat Transfer*, 112:945.

Stewart CW, JM Alzheimer, ME Brewster, G Chen, RE Mendoza, HC Reid, CL Shepard, and G Terrones. 1996. *In Situ Rheology and Gas Volume in Hanford Double-Shell Waste Tanks.* PNNL-11296, Pacific Northwest National Laboratory, Richland, Washington.

Stone WA, DE Jenne, and JM Thorp. 1972. *Climatography of the Hanford Area.* BNWL-1605, Pacific Northwest National Laboratory, Richland, Washington.

Tenekes H and JL Lumley. 1972. *A First Course in Turbulence.* The MIT Press, Cambridge, Massachussetts.

Thurgood MJ. 1996. *Evaluation of Hydrogen Release During Saltwell Pumping for Tanks T-107, S-110, and S-108.* WHC-SD-WM-ER-571 Rev. 0, Westinghouse Hanford Company, Richland, Washington.

Trent DS and LL Eyler. 1991. *TEMPEST, A Computer Program for Three-Dimensional Time-Dependent Hydrothermal Analysis, Vol. 1: User's Manual.* PNWD-1536 Rev. 1, Battelle, Pacific Northwest Laboratories, Richland, Washington.

Wilkins NE. 1996. *Results of Gas Monitoring of Double-Shell Flammable Gas Watch List Tanks.* WHC-SD-WM-TI-682 Rev. 1, Westinghouse Hanford Company, Richland, Washington.

Wilkins NE, RE Bauer, and DM Ogden. 1997. *Results of Vapor Space Monitoring of Flammable Gas Watch List Tanks.* HNF-SD-WM-TI-797 Rev. 1, Lockheed Martin Hanford Corporation, Richland, Washington.

Yoda M, L Hesselink, and MG Mungal. 1994. "Instantaneous Three-Dimensional Concentration Measurements in the Self-Similar Region of a Round High-Schmidt-Number Jet." *J. Fluid Mech.*, v. 279, pp. 313–350.

Distribution

No. of Copies

Offsite

2 DOE Office of Scientific and Technical Information

D. Campbell
102 Windham Road
Oak Ridge, TN 37830

C. W. Forsberg
Oak Ridge National Laboratory
P.O. Box 2008, MS-6495
Oak Ridge, TN 37831-6495

S. J. Eberlein
Westinghouse Savannah River Co.
Savannah River Site, 271-121 H
Aiken, SC 29802

B. Hester
Westinghouse Savannah River Co.
Savannah River Site, 703 H
Aiken, SC 29802

B. C. Hudson
P.O. Box 271
Lindsborg, KS 67456

M. S. Kazimi
Massachusetts Institute
of Technology
Department of Nuclear Engineering
77 Massachusetts Avenue
Cambridge, MA 02139

J. L. Kovach
P.O. Box 29151
70000 Huntley Road
Columbus, OH 43229

T. S. Kress
102-B Newridge Road
Oak Ridge, TN 37830

T. E. Larson
2711 Walnut St.
Los Alamos, NM 87545

No. of Copies

2 Los Alamos National Laboratory
P.O. Box 1663
Los Alamos, NM 87545
Attn: D. Bennett K575
C. Unal K575

D. Pepson
U.S. Department of Energy
Trevion II Building, EM-35
Washington, DC 20585-0002

Scott E. Slezak
806 Hermosa NE
Albuquerque, NM 87110

D. A. Powers
Sandia National Laboratories
MS-0744
Albuquerque, NM 87185-0744

A. B. Stone
Washington Dept. of Ecology
1315 W. 4th, B5-18
Kennewick, WA 99336

J. Tseng
U.S. Department of Energy
Trevion II Building, EM-35
Washington, DC 20585-0002

Onsite

3 DOE Richland Operations Office

C. A. Groendyke S7-54
G. W. Rosenwald S7-54
G. M. Neath S7-51

25 PHMC Team

S. A. Barker R2-11
W. B. Barton R2-11
R. E. Bauer S7-14
D. R. Bratzel S7-14
R. J. Cash S7-14

No. of Copies

PHMC Team (contd)

J. M. Grigsby	S7-14
G. D. Johnson (5)	S7-14
N. W. Kirch	R2-11
J. W. Lentsch	S2-48
R. M. Marusich	A3-34
D. A. Reynolds	R2-11
E. R. Siciliano	HO-31
L. M. Stock	S7-14
R. J. Van Vleet	A3-34
J. R. White	S7-15
N. E. Wilkins	R2-11

No. of Copies

31 Pacific Northwest National Laboratory

Z. I. Antoniak (10)	K7-15
J. M. Bates	K7-15
S. Q. Bennett	K7-90
J. W. Brothers	K5-22
P. A. Gauglitz	P7-41
L. A. Mahoney	K7-15
P. A. Meyer	K7-15
B. J. Palmer	K7-15
L. M. Peurrung	P7-41
K. P. Recknagle	K7-15
H. C. Reid	K7-15
C. W. Stewart (5)	K7-15
G. Terrones	K7-15
Information Release (5)	K6-06